



Robust Participation of Energy Production Companies in the Coupled Gas and Electricity Market Based on Energy Management Strategy

Ali Asghar Baziar¹, Taher Niknam^{1*}, Mohsen Simab¹

¹Department of Electrical Engineering, Marvdasht Branch, Islamic Azad University, Marvdasht, Iran.

Received: 11-Apr-2022, Revised: 29-Jun-2022, Accepted: 16-Jul-2022.

Abstract

This paper presents the optimal participation of strategic electricity and gas producers (SEPs and SGPs) in the coupled electricity and gas market of the day-ahead (DA) reserve regulation and energy type in accordance with the Energy Management Strategy (EMS). The deterministic model of this scheme has two bi-level problems, which refer to modelling of the participation of SEPs/SGPs in the DA energy and reserve markets. In any bi-level problem, the upper-level formulation minimizes the difference between the cost and revenue of SEPs or SGPs in these markets subjected to the operational model of these producers. In the lower-level formulation, the market clearing price (MCP) model is expressed in the problem such that the minimization of the energy cost of non-SEPs / non-SGPs are subjected to the electrical / gas network, electricity / gas generation units, and the reserve requirements model. In this scheme, load, renewable generation power, and reserve demand are uncertain. Hence, this paper proposes the robust modelling to achieve an optimal point in the worst-case scenario. Furthermore, the master-slave decomposition (MSD) method is suggested to reach the optimal solution at a low calculation time. Finally, the proposed scheme is simulated on the standard test system. The numerical results confirm its capability to achieve benefits for SEPs / SGPs along with the extraction of economic operation for energy networks.

Keywords: Coupled Electricity and gas Market, Energy and Reserve Market, Energy Management Strategy, Flexi-Renewable Energy Resources, Strategic Producers.

1. INTRODUCTION

Because of the presence of different

technologies in the field of energy conversion such as gas to power (G2P) or power to gas (P2G), it is expected that the dependency of different energies should be taken into

*Corresponding Authors Email:
niknam@sutech.ac.ir

account in various problems [1]. This is especially evident in the relation between electricity and gas, because electrical energy generation units or power plants generally use gas-fired units (GFUs) due to their appropriate efficiency and lower levels of emission [2]. Moreover, with the influence of fuel cell electric vehicles (FCEVs) in recent years, the use of P2G technologies based on renewable energy sources (RESs) is expected to flourish in the coming years [3]. In addition, the mentioned scheme can be implemented at consumption points, thus the construction cost and strengthening the gas network are avoided. Finally, it should be noted that the extraction of the integrated problem for the simultaneous management of electrical and gas energy can create a variety of capabilities for these energy sources and networks [4-5]. Therefore, from an economic point of view, it is expected that the extraction of a coupled electricity and gas market lead to high efficiency in the economic situation of electricity and gas production companies.

Considering the interdependency of electrical and gas energy, energy management of electrical and gas systems known as multicarrier energy systems or energy hubs has been studied in various research such as [6-10]. In [6], the energy management of hubs in electrical, natural gas, and heat networks is investigated. Since the combined cooling, heat, and power (CCHP) system has been utilized in the hub, the authors in [6] examine the interdependence of electricity, gas, and heat energies. The same paper has also been able to achieve the capability of the energy hub to reduce emissions and energy costs by

defining the model of the two-objective operation problem. A subject similar to the one presented in [6] is also stated in [7], with the difference that the hub in [7] includes different P2G and G2P systems. Authors in [8] show the interdependency of electric, gas, and heat energies resulting from the exploitation of a combined heat and power (CHP) system and a boiler in the hub. In this reference, with the robust operation of the hub in different energy networks, the ability of the hub to improve the operation of the networks and increase the flexibility of the electrical network in the presence of RES has been extracted. The effects of the energy hub on the electrical distribution system have been evaluated under a bi-level operation problem [9]. Following the results obtained in [9], with the energy management of the hub, the minimum operation cost in the distribution network can be obtained. In [10], the ability of the electricity and heat demand response program in the energy hub to improve the operation of different energy networks has been investigated, so that in this case the hub can achieve a flexible network with low operation costs. Additionally, different market models can be defined for energy generation sources. Following this, the day-ahead (DA) energy market for the energy hub in the electricity, gas, and heat markets has been modelled considering the energy price as an uncertainty parameter in [11]. The models of DA energy, real-time (RT), and balancing markets for a virtual power plant (VPP) including wind farm and demand response (DR) are formulated in [12]. Note that in [12], the balancing market considers the cost of imbalance between the DA and RT markets caused by the prediction

error of the generation power by wind farms. This is also presented in [13] except for the energy storage system (ESS) which has also been added to the VPP. As [12-13], in [14], the ESS is flexibility source for wind farms, while in [15] demand response is used as a flexibility source. Also, the coupled DA energy market model of electricity and gas is stated in [16], in which the electricity and gas prices are determined by the market clearing price (MCP) problem, which can consider the dependency on electrical and gas energy prices. Moreover, one of the most important ancillary services in the power system is the reserved service or reserve regulation. Therefore, by using the reserve market, more financial benefits can be obtained for energy generation sources along with their participation in the energy market [17]. Finally, the taxonomy of recent research works is presented in Table 1.

Based on the literature and Table 1, the research gaps in the field of coupled electricity and gas market are as follows:

- Most studies assume the DA energy market model as a parameter for electricity and gas sources by considering energy price as a parameter. Note that, however, due to the existence of G2P and P2G technologies, the prices of gas and electricity energies are expected to be interdependent. Therefore, there is a need to provide a coupled electricity and gas market based on the MCP problem, which is considered in a few studies such as [16].
- It is noteworthy that with proper operation and the use of an appropriate energy management strategy, various capabilities such as reserve services for

generation units and gas producers can be obtained. As a result, they can increase their financial benefit by participating in the coupled electricity and gas ancillary service market along with the coupled energy market of the two mentioned energies, which was not the case in many researches such as [6-16].

- RESs are clean energy generation sources and have low operation costs, so they are important sources of reducing energy price from an economic and social welfare perspective. Note that, these sources have uncertainties in predicting their generation power, so it is possible that the cost of the imbalance between the DA and real-time (RT) markets is high. To address this, it seems appropriate to use a flexi-renewable unit (FRU) that includes a flexible source such as ESS alongside RES. However, it should be noted that this issue has been considered as a single-bus system in most studies such as [12-15] and its effects on the power system have not been studied in many studies.

PM: Proposed model, * Consider the price dependence of gas and electricity networks, # Consider the energy dependence of gas and electricity networks, ** FRU model subject to network constraints.

In line with the first and second research gaps, the participation of strategic electricity and gas producers (SEPs and SGPs) in the DA coupled electricity and gas market, including energy and reserve services, is presented in this paper as shown in Fig. 1. Also, to fill the third research gap, the operation of electrical and natural gas networks in the presence of FRUs is

Table 1. The taxonomy of recent research works.

Ref.	Market type		Consider the price dependence*	Consider the energy dependence [#]	Market model		FRU model**
	Electricity	Gas			Energy	Reserve	
[6]	No	No	No	Yes	No	No	No
[7]	No	No	No	Yes	No	No	No
[8]	No	No	No	Yes	No	No	No
[9]	No	No	No	Yes	No	No	No
[10]	No	No	No	Yes	No	No	No
[11]	Yes	Yes	No	Yes	Yes	No	Yes
[12]	Yes	No	No	No	Yes	No	No
[13]	Yes	No	No	No	Yes	No	No
[14]	Yes	No	No	No	Yes	No	No
[15]	Yes	No	No	No	Yes	No	No
[16]	Yes	Yes	Yes	Yes	Yes	No	No
[17]	Yes	No	No	No	Yes	Yes	No
PM	Coupled gas and electricity markets		Yes	Yes	Yes	Yes	Yes

proportional to the energy management strategy (EMS) in this paper. One should note that flexibility is defined as “*The modification of generation injection and/or consumption patterns in reaction to an external price or activation signal in order to provide a service within the electrical system*” [18]. Therefore, ESS as a flexible source alongside RES can be improved FRU flexibility using a suitable EMS model [18]. In the remaining, the deterministic model of the proposed scheme has a bi-level problem for the participation of SEPs including GFU, non-GFU (NGFU), and FRU in DA energy and reserve markets, and a bi-level problem

for the participation of SGPs including P2G and gas well (GW) in the mentioned markets. In each of the problems, the upper-level formulation contains an objective function aiming to minimize the difference between the cost and revenue of SEPs or SGPs in the DA energy and reserve markets. The lower-level problem has the MCP model, which has an objective function to minimize the operation costs of non-SEPs/non-SGPs. non-SEPs include GFU, NGFU, and FRU, and non-SGPs include GW and P2G. It is also subjected to electricity/gas power flow constraints, models of generation units/gas producers, and formulation of reserve

services in the electricity/gas system. Note that in these problems, the load, RES output power, and reserve demand have uncertainties. In this paper, robust modelling is used to achieve the optimal robust point in the worst-case scenario resulting from these uncertainties. In addition, it should be said that in the coupled electricity and gas market model, the demand for input active power of the P2G and the fuel price of the GFU are determined from the gas market as shown in Fig. 1, and the demand for input gas power of the GFU and operation price of the P2G are obtained from the electricity market. Consequently, the two bi-level problems expressed are not independent of each other, but have a non-integrated format. In other words, the scheme is in line with the decomposition solution framework. Thus, in this paper, the master-slave decomposition (MSD) algorithm is employed to achieve the optimal solution in the shortest possible time. Finally, the contributions of the proposed scheme are described as follows: Presenting a model for the optimization problem of the participation of SEPs and SGPs in the coupled electricity and gas market with DA energy and reserve services to estimate the dependence of different parameters in the field of electricity and gas;

- Using an energy management strategy for electricity and gas networks in the presence of FRU to achieve a flexible network with clean energy with high social efficiency with a reduction in energy prices;
- Achieving a robust optimal point in the worst-case scenario due to uncertainties

in demand and supply by using -robust modelling; and

- Using the MSD algorithm to achieve the optimal solution in the shortest possible time for problems with a non-integrated optimization format.

The paper is organized as follows: Section 2 presents the deterministic model of the participation of SEPs and SGPs in the coupled electricity and gas market and Section 3 describes its robust model. The solution process based on the MSD algorithm is mentioned in Section 4, and finally, the numerical results and conclusions are presented in Sections 5 and 6, respectively.

2. FORMULATION OF THE PROPOSED PROBLEM

2.1. Electricity Market Model

This section provides the optimal participation model of SEPs in the DA electrical energy and reserve market as a bi-level problem, in the upper level of which the SEPs participation in the mentioned markets with minimizing the difference between their cost and revenue is considered. Also, in the lower level formulation, the MCP model in the mentioned markets is based on the electricity transmission network model. In this problem, the minimization of the operation cost of the non-SEPs is constrained to DC optimal power flow (DC-OPF) equations, non-SEPs models including the FRU, GFU, and NGFU, and reserve requirement constraints of the network. Thus, the proposed problem is written as follows:

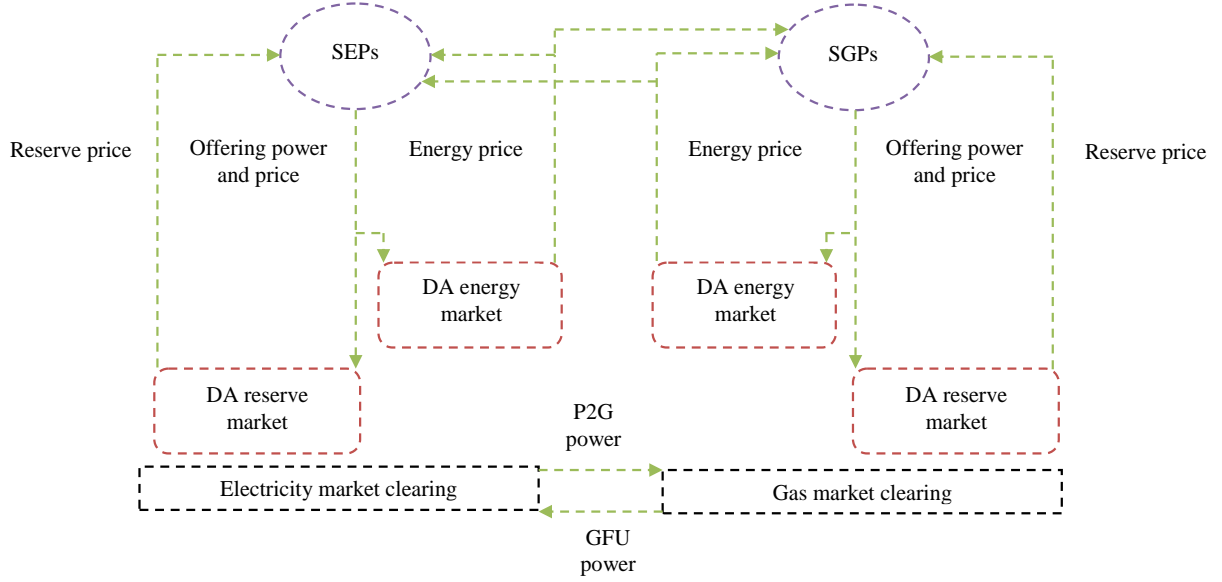


Fig. 1. The framework of the proposed scheme.

$$\min \sum_{i \in \Psi_{Gs}} \sum_{t \in \Psi_T} \left(\beta_i (P_{Gi,t} + RU_{Gi,t} + RD_{Gi,t}) + \frac{1}{\eta_i} (P_{Gi,t} + RU_{Gi,t} + RD_{Gi,t}) \sum_{g \in \Psi_N} B_{g,i} \lambda_{g,t}^{GE} \right) - \sum_{b \in \Psi_B} \sum_{t \in \Psi_T} \left(\lambda_{b,t}^{EE} \sum_{i \in \Psi_{Gs}} A_{b,i} P_{Gi,t} + \lambda_{b,t}^{EU} \sum_{i \in \Psi_{Gs}} A_{b,i} RU_{Gi,t} + \lambda_{b,t}^{ED} \sum_{i \in \Psi_{Gs}} A_{b,i} RD_{Gi,t} \right) \quad (1)$$

Subject to:

$$\underline{P}_{Gi,t} \leq P_{Gi,t} \leq \bar{P}_{Gi,t} \quad \forall i \in \Psi_{Gs}, t \quad (2)$$

$$P_{Gi,t} + RU_{Gi,t} \leq \bar{P}_{Gi,t} \quad \forall i \in \Psi_{Gs}, t \quad (3)$$

$$\underline{P}_{Gi,t} \leq P_{Gi,t} - RD_{Gi,t} \quad \forall i \in \Psi_{Gs}, t \quad (4)$$

$$RU_{Gi,t} \geq 0 \quad \forall i \in \Psi_{Gs}, t \quad (5)$$

$$RD_{Gi,t} \geq 0 \quad \forall i, t \quad (6)$$

$$P_{Gi,t} = P_{Wi,t} + (P_{Di,t} - P_{Ci,t}) \quad \forall i \in \Psi_{Gs}^{FR}, t \quad (7)$$

$$0 \leq P_{Di,t} \leq DR_i \quad \forall i \in \Psi_{Gs}^{FR}, t \quad (8)$$

$$0 \leq P_{Ci,t} \leq CR_i \quad \forall i \in \Psi_{Gs}^{FR}, t \quad (9)$$

$$\underline{E}_i \leq E_i(0) + \sum_{\tau=1}^t \left(\eta_{Ci} P_{Ci,\tau} - \frac{1}{\eta_{Di}} P_{Di,\tau} \right) \leq \bar{E}_i \quad \forall i \in \Psi_{Gs}^{FR}, t \quad (10)$$

$$\lambda^{EE}, \lambda^{EU}, \lambda^{ED} \in \arg \left\{ \min \sum_{i \in (\Psi_G - \Psi_{Gs})} \sum_{t \in \Psi_T} \left(\beta_i (P_{Gi,t} + RU_{Gi,t} + RD_{Gi,t}) + \frac{1}{\eta_i} (P_{Gi,t} + RU_{Gi,t} + RD_{Gi,t}) \sum_{g \in \Psi_N} B_{g,i} \lambda_{g,t}^{GE} \right) \right\} \quad (11)$$

Subject to:

$$\sum_{i \in \Psi_G} A_{b,i} P_{Gi,t} - \sum_{l \in \Psi_L} C_{b,l} P_{Ll,t} = P_{Db,t} + \quad (12)$$

$$\sum_{j \in \Psi_{2G}^{pg}} \frac{1}{\eta_j} F_{b,j} (Q_{Sj,t} + RU_{Sj,t} + RD_{Sj,t}) : \lambda_{b,t}^{EE} \quad \forall b, t$$

$$P_{Ll,t} = B_{Ll} \sum_{b \in \Psi_B} C_{b,l} \delta_{b,t} : \lambda_{l,t}^{pl} \quad \forall l, t \quad (13)$$

$$\delta_{b,t} = 0 : \lambda_q^{\delta} \quad \forall b = \text{Slack bus}, t \quad (14)$$

$$-\bar{P}_{Ll} \leq P_{Ll,t} \leq \bar{P}_{Ll} : \underline{\mu}_{l,t}^{pl}, \bar{\mu}_{l,t}^{pl} \quad \forall l, t \quad (15)$$

$$\underline{P}_{Gi,t} \leq P_{Gi,t} \leq \bar{P}_{Gi,t} : \underline{\mu}_{i,t}^{pg}, \bar{\mu}_{i,t}^{pg} \quad \forall i \in (\Psi_G - \Psi_{Gs}), t \quad (16)$$

$$P_{Gi,t} + RU_{Gi,t} \leq \bar{P}_{Gi,t} : \bar{\mu}_{i,t}^{ru} \quad \forall i \in (\Psi_G - \Psi_{Gs}), t \quad (17)$$

$$\underline{P}_{Gi,t} \leq P_{Gi,t} - RD_{Gi,t} : \underline{\mu}_{i,t}^{rd} \quad \forall i \in (\Psi_G - \Psi_{Gs}), t \quad (18)$$

$$RU_{Gi,t} \geq 0 : \underline{\mu}_{i,t}^{rug} \quad \forall i \in (\Psi_G - \Psi_{Gs}), t \quad (19)$$

$$RD_{Gi,t} \geq 0 : \underline{\mu}_{i,t}^{rdg} \quad \forall i \in (\Psi_G - \Psi_{Gs}), t \quad (20)$$

$$P_{Gi,t} = P_{Wi,t} + (P_{Di,t} - P_{Ci,t}) : \lambda_{i,t}^{fn} \quad \forall i \in (\Psi_G^{FR} - \Psi_{Gs}^{FR}), t \quad (21)$$

$$0 \leq P_{Di,t} \leq DR_i : \underline{\mu}_{i,t}^{pd}, \bar{\mu}_{i,t}^{pd} \quad \forall i \in (\Psi_G^{FR} - \Psi_{Gs}^{FR}), t \quad (22)$$

$$0 \leq P_{Ci,t} \leq CR_i : \underline{\mu}_{i,t}^{pc}, \bar{\mu}_{i,t}^{pc} \quad \forall i \in (\Psi_G^{FR} - \Psi_{Gs}^{FR}), t \quad (23)$$

$$\underline{E}_i \leq E_i(0) + \sum_{\tau=1}^t \left(\eta_{Ci} P_{Ci,\tau} - \frac{1}{\eta_{Di}} P_{Di,\tau} \right) \leq \bar{E}_i : \underline{\mu}_{i,t}^e, \bar{\mu}_{i,t}^e \quad \forall i \in (\Psi_G^{FR} - \Psi_{Gs}^{FR}), t \quad (24)$$

$$\sum_{i \in \Psi_G} A_{b,i} RU_{Gi,t} = UR_{Eb,t} : \lambda_{b,t}^{EU} \quad \forall b,t \quad (25)$$

$$\left. \sum_{i \in \Psi_G} A_{b,i} RD_{Gi,t} = DR_{Eb,t} : \lambda_{b,t}^{ED} \quad \forall b,t \right\} \quad (26)$$

The upper-level problem refers to SEPs participation in the DA energy and reserve markets; hence, equation (1) considers minimizing the difference between the cost and revenue of SEPs in the proposed markets as the objective function for this level [18]. SEP revenue in these markets obtains from the sale of energy in the energy market [19] and the presence of service in the reserve market. Equations (2)-(10) provide the constraints of SEPs in the upper-level problem, so that the capability curve of their generation unit is presented in Eq. (2), which indicates the limit of active power generation of SEPs [20]. Constraints (3) and (4) also represent the limitation of the output power of the mentioned sources considering their reserve power generation. Hence, using the (3) or (4), the amount of up or down reserve power can be calculated, so that these variables always have a positive value based on constraints (5) and (6) [21]. In (7) to (10), the SEPs model is of FRU type. In Eq. (7), the power balance in this unit is modelled. Equations (8) and (9) state the charging and discharging rate limits of the ESS in this unit, respectively [18]. Finally, the storage energy limit in the ESS of this SEP is expressed in (10) [18]. According to Eq. (7), the net output power of FRU is equal to the sum of the power of the wind farm and ESS, so its charge/discharge power appears with a negative/positive sign in the mentioned equation. Also, in this problem, it is assumed

that the ESS in a FRU will be charged only by the wind farm of that FRU, so the minimum output power of the FRU in constraint (2) will be zero.

The local electricity marginal price (LEMP) of energy and reserve services, λ^{EE} , λ^{EU} and λ^{ED} , can be obtained from the MCP problem [19]; hence, the lower-level problem or the MCP with a model described by (11)-(26) is added to the upper-level problem. In this problem, Eq. (11) represents the objective function of the MCP strategy, i.e., minimizing the operation costs of non-SEPs including GFUs and NFGUs. In the first term of the mentioned equation, the fuel cost of the non-SEPs with NGFU type includes active and reserve power, the fuel price of which has a fixed value for all simulation hours. In the second part of Eq. (11), the operation cost of non-SEPs with GFU type for active and reserve powers is stated. This cost for a GFU depends on the gas price of the gas node to which the GFU is connected [16]. It is noteworthy that in the FRU, the very low operation cost of renewable resources can be neglected. It is also assumed that the ESS in this generation unit is charged by RES generation power. Therefore, the operation cost of these power sources is negligible, so variables of this type of non-SEPs will not be available in the objective function (11). The conditions for SEPs are stated in the first term of Eq. (1). In the following, the DC-OPF constraints are given in Eqs. (12) to (15),

which represent the active power balance on each bus, the active power flowing through the transmission line, the slack bus voltage, and the technical limit of the system, i.e., the limitation of power flow in the transmission line [20]. In Eq. (12), the amount of load consumed in a bus is equal to the total passive load of that bus and the electrical power required by P2Gs in that bus [16]. Equations (16)-(24) are the same with constraints (2)-(10), but these equations are related to the non-SEPs model. Ultimately, the up and down reserve demands in each bus will be based on rules (25) and (26), respectively. Based on these relationships, the reserve demand for each bus is met by the SEPs or non-SEPs on that bus. Moreover, the

variables μ or λ for an equation represent the Lagrangian multipliers of that equation.

2.2. Gas Market Model

The problem of optimal participation of SGPs in the DA gas energy and reserve markets is presented in this section. It is a bi-level problem that, at the upper level, expresses the minimization of the difference between the cost and revenue of SGPs in these markets subject to the SGPs operation model. Also, the MCP model in these markets is constrained to the natural gas network model by minimizing the operation cost of non-SGPs at the lower level of the problem. Therefore, the model of the problem will be as follows:

$$\min \sum_{j \in \Psi_{W_s}} \sum_{t \in \Psi_T} \left(\alpha_j (Q_{S_{j,t}} + RU_{S_{j,t}} + RD_{S_{j,t}}) + \frac{1}{\eta_j} (Q_{S_{j,t}} + RU_{S_{j,t}} + RD_{S_{j,t}}) \sum_{b \in \Psi_B} F_{b,j} \lambda_{b,t}^{EE} \right) - \sum_{g \in \Psi_N} \sum_{t \in \Psi_T} \left(\lambda_{g,t}^{GE} \sum_{j \in \Psi_{W_s}} D_{g,j} Q_{S_{j,t}} + \lambda_{g,t}^{GU} \sum_{j \in \Psi_{W_s}} D_{g,j} RU_{S_{j,t}} + \lambda_{g,t}^{GD} \sum_{j \in \Psi_{W_s}} D_{g,j} RD_{S_{j,t}} \right) \quad (27)$$

Subject to:

$$\underline{Q}_{S_{j,t}} \leq Q_{S_{j,t}} \leq \bar{Q}_{S_{j,t}} \quad \forall j \in \Psi_{W_s}, t \quad (28)$$

$$Q_{S_{j,t}} + RU_{S_{j,t}} \leq \bar{Q}_{S_{j,t}} \quad \forall j \in \Psi_{W_s}, t \quad (29)$$

$$\underline{Q}_{S_{j,t}} \leq Q_{S_{j,t}} - RD_{S_{j,t}} \quad \forall j \in \Psi_{W_s}, t \quad (30)$$

$$RU_{S_{j,t}} \geq 0 \quad \forall j \in \Psi_{W_s}, t \quad (31)$$

$$RD_{S_{j,t}} \geq 0 \quad \forall j \in \Psi_{W_s}, t \quad (32)$$

$$\lambda^{GE}, \lambda^{GU}, \lambda^{GD} \in \arg \left\{ \min \sum_{j \in (\Psi_W - \Psi_{W_s})} \sum_{t \in \Psi_T} \left(\alpha_j (Q_{S_{j,t}} + RU_{S_{j,t}} + RD_{S_{j,t}}) + \frac{1}{\eta_j} (Q_{S_{j,t}} + RU_{S_{j,t}} + RD_{S_{j,t}}) \sum_{b \in \Psi_B} F_{b,j} \lambda_{b,t}^{EE} \right) \right\} \quad (33)$$

Subject to:

$$\sum_{j \in \Psi_W} D_{g,j} Q_{S j,t} - \sum_{p \in \Psi_P} H_{g,p} Q_{P p,t} = Q_{D g,t} + \quad (34)$$

$$\sum_{i \in \Psi_G^{G2P}} \frac{1}{\eta_i} B_{g,i} (P_{G i,t} + RU_{G i,t} + RD_{G i,t}) : \lambda_{g,t}^{GE} \quad \forall g,t$$

$$\Delta \gamma_{p,t,k} = \frac{m_k^\sigma}{m_k^\gamma} \sum_{g \in \Psi_N} H_{g,p} \Delta \sigma_{g,t,k} : \lambda_{p,t,k}^{\Delta \gamma} \quad \forall p,t,k \quad (35)$$

$$Q_{P p,t} = \kappa_{P p} \sum_{k \in \Psi_K} \Delta \gamma_{p,t,k} : \lambda_{p,t}^{qp} \quad \forall p,t \quad (36)$$

$$\sigma_{g,t} = \underline{\sigma} + \sum_{k \in \Psi_K} \Delta \sigma_{g,t,k} : \lambda_{g,t}^{\Delta \sigma} \quad \forall g,t \quad (37)$$

$$\sigma_{g,t} = 1 : \lambda_t^\sigma \quad \forall g = \text{Slack node}, t \quad (38)$$

$$-\bar{Q}_{P p} \leq Q_{P p,t} \leq \bar{Q}_{P p} : \underline{\mu}_{p,t}^{qp}, \bar{\mu}_{p,t}^{qp} \quad \forall p,t \quad (39)$$

$$\underline{\sigma} \leq \sigma_{g,t} \leq \bar{\sigma} : \underline{\mu}_{g,t}^\sigma, \bar{\mu}_{g,t}^\sigma \quad \forall g,t \quad (40)$$

$$\underline{Q}_{S j,t} \leq Q_{S j,t} \leq \bar{Q}_{S j,t} : \underline{\mu}_{j,t}^{qs}, \bar{\mu}_{j,t}^{qs} \quad \forall j \in (\Psi_W - \Psi_{Ws}), t \quad (41)$$

$$Q_{S j,t} + RU_{S j,t} \leq \bar{Q}_{S j,t} : \bar{\mu}_{j,t}^{rus} \quad \forall j \in (\Psi_W - \Psi_{Ws}), t \quad (42)$$

$$\underline{Q}_{S j,t} \leq Q_{S j,t} - RD_{S j,t} : \underline{\mu}_{j,t}^{rds} \quad \forall j \in (\Psi_W - \Psi_{Ws}), t \quad (43)$$

$$RU_{S j,t} \geq 0 : \underline{\mu}_{j,t}^{rups} \quad \forall j \in (\Psi_W - \Psi_{Ws}), t \quad (44)$$

$$RD_{S j,t} \geq 0 : \underline{\mu}_{j,t}^{rdps} \quad \forall j \in (\Psi_W - \Psi_{Ws}), t \quad (45)$$

$$\sum_{j \in \Psi_W} D_{g,j} RU_{S j,t} = UR_{G g,t} : \lambda_{g,t}^{GU} \quad \forall g,t \quad (46)$$

$$\left. \sum_{j \in \Psi_W} D_{g,j} RD_{S j,t} = DR_{G g,t} : \lambda_{g,t}^{GD} \quad \forall g,t \right\} \quad (47)$$

The upper-level problem has a model, Eqs. (27)-(32), which refers to the SGPs participation in the DA gas energy and reserves markets [16]. Eq (27) is the objective function of this problem, where it

minimizes the difference between the cost and revenue of SGPs in the mentioned markets [16]. The constraints of SGPs are mentioned in (28) to (32), so that the limit on the gas generation of each SGP is given by

(28) [16]. Also, this limitation is presented by considering up and down gas reserves in (29) and (20). In addition, these constraints can be used to calculate the gas power of up and down reserves, respectively, so these variables should be positive as constraints (31) and (32).

Similar to the problem described by (1)-(26), the local gas marginal price (LGMP) in DA energy, up and down reserve markets, λ^{GE} , λ^{GU} and λ^{GD} , are calculated by the MCP problem in the lower level problem, which has a similar model as given in (33)-(47) [16]. Equation (33) represents the objective function of the MCP scheme in the natural gas network, which aims to minimize the operation cost of non-SGPs including GW and P2G. The first term of the function denotes the operation cost of the GWs to generate gas energy and provide reserve services, which is in proportion to the fixed price at all simulation hours. Also, the second term in (33) refers to the P2Gs operation cost in gas energy production and providing reserve services, where the purchase price of the input energy in a P2G as given in Eq. (33) depends on the LEMP of energy in the electrical bus with a connected P2G [16]. There are these conditions for SGPs according to the first of Eq. (27). Moreover, constraints related to the natural gas network are presented in Eqs. (34)-(40). Equation (34) expresses the balance of gas power in each node, where the demand for gas power in each node is the result of the passive gas load in that node and the input gas power of the GFUs connected to the node. The gas power flowing through each gas pipe is calculated based on linear constraints (35)-(37). Note that this variable has a nonlinear relationship

as $Q_p = \kappa_p \sqrt{(\sigma_x)^2 - (\sigma_y)^2}$ [11], the amount of which depends on the gas pressure at both ends of a pipeline. Therefore, to achieve the linear model, first, this relation is considered as $Q_p = \kappa_p \gamma_p$, where γ is an auxiliary variable that can be calculated from $\gamma^2 = (\sigma_x)^2 - (\sigma_y)^2$. Now, $\gamma^2 = (\sigma_x)^2 - (\sigma_y)^2$ can be expressed as a linear relationship as described by (35) using the conventional piecewise linear technique [11]. It should be noted that, in this case, γ will be $\sum_{k \in \Psi_k} \Delta \gamma_{p,t,s,k}$, so $Q_p = \kappa_p \gamma_p$ is modelled as a linear constraint (36). Finally, based on the mentioned linearization technique, the pressure variable (σ) will be as (37) [11]. Next, the corresponding pressure constraint on the slack node will be as (38). Furthermore, constraints (39) and (40) express the technical limitations of the natural gas network, such as the constraint on the capacity of the pipeline and the gas pressure of the nodes [11]. The constraints of non-SGPs are mentioned in Eqs. (41)-(45) that are included the same format with constraints (28)-(32). Finally, the up and down gas reserve requirements in the natural gas network nodes that have SGPs or non-SGPs are in accordance with (46) and (47), respectively. Also, the variables μ or λ for an equation represent the Lagrangian multipliers of that equation.

Note that in the upper-level problem, the goal is to maximize the profits of energy producers, and that model has considered the performance of these producers. However, in the case of the lower-level problem, the goal of the network operator is to promote social welfare. Therefore, it considers minimizing

the cost of energy generation as an objective function. Thus, the models used for objective functions of upper and lower-level problems are different.

3. ROBUST PARTICIPATION OF SEPS AND SGPS IN THE COUPLED ELECTRICAL AND GAS MARKET

In problems (1)-(26) and (27)-(47), parameters such as load, P_D and Q_D , wind farm power, P_W , active and gas reserve demand, UR_E , DR_E , UR_G , and DR_G are uncertain. Therefore, probabilistic, stochastic, and robust modelling should be performed for the proposed problems. However, it should be noted that in the probabilistic and stochastic model, it is necessary to identify the probability distribution function (PDF) of each uncertainty parameter. Since obtaining an accurate PDF requires statistical information over a long study period such as one year, this will be very time-demanding. Additionally, to achieve a guaranteed optimal solution in this type of modelling, the proposed scheme needs to be implemented in a significant number of scenarios, so it is expected that the problem solving time is high [22]. Therefore, to compensate for these challenges, robust modelling is used for the proposed problems in this paper, which has only one scenario, known as the “*worst-case scenario*” [22]. It should also be said that the optimal solution position in other scenarios will be more favourable than the optimal situation in the robust model [22]. In this paper, it is assumed that the true value of an uncertainty parameter u is in the range $[(1-\zeta)\times\bar{u}, (1+\zeta)\times\bar{u}]$, in which \bar{u} represents the predicted value of

the parameter u , and ζ is the forecasted error [18]. Hence, since the model of problems (1)-(26) and (27)-(47) is linear programming (LP), it is expected that the true value of each uncertainty parameter in the worst-case scenario is equal to its upper or lower limit [18]. It is noteworthy that in the robust model, the feasibility region will be smaller than in the deterministic model because the worst case scenario is used in this modelling. Therefore, the true value of u depends on the location of the parameter u and its coefficient (-1 or +1), and the type of objective function i.e. max or min [18]. For example, in order to minimize the feasibility region of the problem (1)-(26) in the worst-case scenario compared to the scenario related to the deterministic model, the true values of P_D , UR_E , and DR_E must be equal to their upper-limit, while the true value of P_W is on its lower limit because the positions of P_D , UR_E and DR_E in the balance constraints, i.e. (12), (25), and (26), are on the right side of the equation with a positive coefficient. Also, since the objective function (11) is of type min, increasing the values of these parameters in the robust model compared to the deterministic model causes the non-SEPs to produce more power. This means an increase in the value of the objective function (11) in the robust model compared to the deterministic model, which is due to the reduction of the solution space in the worst case scenario compared to the scenario corresponding to the deterministic model. The opposite is true for P_W , so its true value is on its lower limit. Moreover, it should be said that the model of the problem (27)-(47) is the same as the problem (1)-(26), except that it is expressed in the natural gas network.

Consequently, the true values of Q_D , UR_G , and DR_G are at their higher limits like P_D , UR_E , and DR_E . Therefore, a robust model of the mentioned problems will be presented as follows:

- A robust model of SEPs participation in the electrical energy and reserve markets

Problem (1)-(26) considering (48)

$$P_{Db,t}(1+\varphi), UR_{Eb,t}(1+\varphi), DR_{Eb,t}(1+\varphi)$$

and $P_{Wi,t}(1-\varphi)$ instead of $P_{Db,t}$, $UR_{Eb,t}$, $DR_{Eb,t}$ and $P_{Wi,t}$, respectively.

- A robust model of SGPs participation in the gas energy and reserves markets

Problem (27)-(47) considering (49)

$$Q_{Dg,t}(1+\varphi), UR_{Gg,t}(1+\varphi) \text{ and } DR_{Gg,t}(1+\varphi)$$

instead of $Q_{Dg,t}$, $UR_{Gg,t}$ and $DR_{Gg,t}$, respectively.

4. SOLUTION METHOD

4.1. Integrated Model

Problems (48) and (49) are bi-level optimization problems with the following standard format:

$$\max F_1(y, \lambda, \mu) \quad (50)$$

$$G_1(y) = 0 \quad (51)$$

$$G_2(y) = 0 \quad (52)$$

Subject to:

$$\{\min F_2(y) \quad (53)$$

Subject to:

$$G_3(y) = 0 : \lambda \quad (54)$$

$$G_4(y) \leq 0 : \mu \quad (55)$$

In this model, y represents the variables

of the primal problem (48) or (49), and λ and μ are Lagrange multipliers. F_1 and F_2 are the objective functions of the upper and lower-level problems. Constraints (51)/(54) and (52)/(55) represent the balance constraints and limitations in the formulation of Sections 1.2 or 2.2, respectively. To achieve an integrated or single-level model for the bi-level model (50)-(55), this paper employs the Karush-Kuhn-Tucker (KKT) method [19]. In this method, the KKT model related to lower-level problem is added to the upper-level problem, which will eventually form a single-objective problem. To obtain the KKT model, the Lagrange function of the lower-level problem based on [19] is first written as follows:

$$L(y, \lambda, \mu) = F_2(y) + \lambda G_3(y) + \mu \max(0, G_4(y)) \quad (56)$$

Then, according to the proposed method, the integrated or single-objective problem model is presented as follows, where equations (57)-(58) / (59)-(62) are upper-level problem / KKT model:

$$\max F_1(y, \lambda, \mu) \quad (57)$$

$$\text{Constraints (51)-(52)} \quad (58)$$

Subject to:

$$\frac{\partial F_2}{\partial y} + \lambda \frac{\partial G_1}{\partial y} + \mu \frac{\partial G_2}{\partial y} = 0 : \frac{\partial L}{\partial y} = 0 \quad (59)$$

$$G_3(y) = 0 : \frac{\partial L}{\partial \lambda} = 0 \quad (60)$$

$$G_4(y) \leq 0, \mu G_4(y) = 0 : \frac{\partial L}{\partial \mu} = 0 \quad (61)$$

$$\lambda \in (-\infty, +\infty), \mu \in [0, +\infty) \quad (62)$$

In the above problem, the objective

function of the new problem (57) is equal to the objective function of the upper-level problem (50). Equation (58) is same with upper level constraints, and constraints (59) to (61) are obtained from $\frac{\partial L}{\partial y} = 0$, $\frac{\partial L}{\partial \lambda} = 0$ and $\frac{\partial L}{\partial \mu} = 0$, respectively. Constraint (62) also indicates the range of changes in Lagrange multipliers. In addition, in (61), the equation $\mu G_2(y)$ is nonlinear. To linearize it, $-M.(1-z) \leq G_2(y) \leq 0$ and $0 \leq \mu \leq M.z$ are substituted for this equation, where z represents an auxiliary binary variable, and M

is a constant with a large value such as 10^6 [19].

The second term of objectives (1) and (27) will have a non-linear format in the single-level problem due to the multiplication of primary (y) and dual (λ) variables. This non-linear equation can be converted to linear formulation using the strong duality method [16]. In this approach, the objective function of the lower-level problem, i.e. (11) or (33), is equal respectively to (63) and (64) that are presented the objective function in the dual model of this problem [16]. Hence, the non-linear term of equations (1) and (27) will be written as (65) and (66), respectively.

$$\begin{aligned} & \sum_{b,t} \left\{ \lambda_{b,t}^{EE} \left((1+\zeta) P_{D_{b,t}} + \sum_{j \in \Psi_W^{p2G}} \frac{1}{\eta_j} F_{b,j} (Q_{S_{j,t}} + RU_{S_{j,t}} + RD_{S_{j,t}}) - \sum_{i \in \Psi_{G_s}} A_{b,i} P_{G_{i,t}} \right) + \right. \\ & \left. \left((1+\zeta) UR_{E_{b,t}} - \sum_{i \in \Psi_{G_s}} A_{b,i} RU_{G_{i,t}} \right) \lambda_{b,t}^{EU} + \left((1+\zeta) DR_{E_{b,t}} - \sum_{i \in \Psi_{G_s}} A_{b,i} RD_{G_{i,t}} \right) \lambda_{b,t}^{ED} \right\} + \\ & \sum_{l,t} \bar{P}_{Ll} \left(\bar{\mu}_{l,t}^{pl} - \underline{\mu}_{l,t}^{pl} \right) + \sum_{i \in (\Psi_G - \Psi_{G_s}),t} \left\{ \underline{P}_{G_{i,t}} \underline{\mu}_{i,t}^{pg} + \bar{P}_{G_{i,t}} \bar{\mu}_{i,t}^{pg} + \bar{P}_{G_{i,t}} \bar{\mu}_{i,t}^{ru} + \underline{P}_{G_{i,t},s} \underline{\mu}_{i,t}^{rd} \right\} \\ & + \sum_{i \in (\Psi_G^{FR} - \Psi_{G_s}^{FR}),t} \left\{ (1-\zeta) P_{W_{i,t}} \lambda_{i,t}^{fru} + DR_i \bar{\mu}_{i,t}^{pd} + CR_i \bar{\mu}_{i,t}^{pc} + (\underline{E}_i - E_i(0)) \underline{\mu}_{i,t}^e + (\bar{E}_i - E_i(0)) \bar{\mu}_{i,t}^e \right\} \end{aligned} \quad (63)$$

$$\begin{aligned} & \sum_{g,t} \left\{ \lambda_{g,t}^{GE} \left((1+\zeta) Q_{D_{g,t}} + \sum_{i \in \Psi_G^{G2P}} \frac{1}{\eta_i} B_{g,i} (P_{G_{i,t}} + RU_{G_{i,t}} + RD_{G_{i,t}}) - \sum_{j \in \Psi_{W_s}} D_{g,j} Q_{S_{j,t}} \right) + \right. \\ & \left. \lambda_{g,t}^{GU} \left((1+\zeta) UR_{G_{g,t}} - \sum_{j \in \Psi_{W_s}} D_{g,j} RU_{S_{j,t}} \right) + \lambda_{g,t}^{GD} \left((1+\zeta) DR_{G_{g,t}} - \sum_{j \in \Psi_{W_s}} D_{g,j} RD_{S_{j,t}} \right) + \underline{\sigma} \cdot \lambda_{g,t}^{\Delta\sigma} + \underline{\sigma} \cdot \underline{\mu}_{g,t}^{\sigma} + \bar{\sigma} \cdot \bar{\mu}_{g,t}^{\sigma} \right\} + \\ & \sum_t \lambda_t^{\sigma} + \sum_{p,t} \bar{Q}_{pp} \left(\bar{\mu}_{p,t}^{qp} - \underline{\mu}_{p,t}^{qp} \right) + \sum_{j \in (\Psi_W - \Psi_{W_s}),t} \left\{ \underline{Q}_{S_{j,t}} \underline{\mu}_{j,t}^{qs} + \bar{Q}_{S_{j,t}} \bar{\mu}_{j,t}^{qs} + \bar{Q}_{S_{j,t}} \bar{\mu}_{j,t}^{rus} + \underline{Q}_{S_{j,t}} \underline{\mu}_{j,t}^{rds} \right\} \end{aligned} \quad (64)$$

$$\begin{aligned}
& \sum_{b \in \Psi_B} \sum_{t \in \Psi_T} \left(\lambda_{b,t}^{EE} \sum_{i \in \Psi_{G_s}} A_{b,i} P_{G_i,t} + \lambda_{b,t}^{EU} \sum_{i \in \Psi_{G_s}} A_{b,i} R U_{G_i,t} + \lambda_{b,t}^{ED} \sum_{i \in \Psi_{G_s}} A_{b,i} R D_{G_i,t} \right) = \\
& \sum_{i \in (\Psi_G - \Psi_{G_s})} \sum_{t \in \Psi_T} \left(\beta_i (P_{G_i,t} + R U_{G_i,t} + R D_{G_i,t}) + \frac{1}{\eta_i} (P_{G_i,t} + R U_{G_i,t} + R D_{G_i,t}) \sum_{g \in \Psi_N} B_{g,i} \lambda_{g,t}^{GE} \right) - \\
& \left\{ \sum_{b,t} \left\{ \lambda_{b,t}^{EE} \left((1+\zeta) P_{D_b,t} + \sum_{j \in \Psi_{P2G}} \frac{1}{\eta_j} F_{b,j} (Q_{S j,t} + R U_{S j,t} + R D_{S j,t}) \right) + ((1+\zeta) U R_{E_b,t}) \lambda_{b,t}^{EU} + ((1+\zeta) D R_{E_b,t}) \lambda_{b,t}^{ED} \right\} + \right. \\
& \left. \sum_{l,t} \bar{P}_{Ll} (\bar{\mu}_{l,t}^{pl} - \underline{\mu}_{l,t}^{pl}) + \sum_{i \in (\Psi_G - \Psi_{G_s}),t} \left\{ \underline{P}_{G_i,t} \underline{\mu}_{i,t}^{pg} + \bar{P}_{G_i,t} \bar{\mu}_{i,t}^{pg} + \bar{P}_{G_i,t} \bar{\mu}_{i,t}^{ru} + \underline{P}_{G_i,t} \underline{\mu}_{i,t}^{rd} \right\} + \right. \\
& \left. \sum_{i \in (\Psi_G^{FR} - \Psi_{G_s}^{FR}),t} \left\{ (1-\zeta) P_{W_i,t} \lambda_{i,t}^{fru} + D R_i \bar{\mu}_{i,t}^{pd} + C R_i \bar{\mu}_{i,t}^{pc} + (E_i - E_i(0)) \underline{\mu}_{i,t}^e + (\bar{E}_i - E_i(0)) \bar{\mu}_{i,t}^e \right\} \right\}
\end{aligned} \tag{65}$$

$$\begin{aligned}
& \sum_{g \in \Psi_N} \sum_{t \in \Psi_T} \left(\lambda_{g,t}^{GE} \sum_{j \in \Psi_{W_s}} D_{g,j} Q_{S j,t} + \lambda_{g,t}^{GU} \sum_{j \in \Psi_{W_s}} D_{g,j} R U_{S j,t} + \lambda_{g,t}^{GD} \sum_{j \in \Psi_{W_s}} D_{g,j} R D_{S j,t} \right) = \\
& \sum_{j \in (\Psi_W - \Psi_{W_s})} \sum_{t \in \Psi_T} \left(\alpha_j (Q_{S j,t} + R U_{S j,t} + R D_{S j,t}) + \frac{1}{\eta_j} (Q_{S j,t} + R U_{S j,t} + R D_{S j,t}) \sum_{b \in \Psi_B} F_{b,j} \lambda_{b,t}^{EE} \right) - \\
& \left\{ \sum_{g,t} \left\{ \lambda_{g,t}^{GE} \left((1+\zeta) Q_{D g,t} + \sum_{i \in \Psi_{G2P}} \frac{1}{\eta_i} B_{g,i} (P_{G_i,t} + R U_{G_i,t} + R D_{G_i,t}) \right) + \lambda_{g,t}^{GU} ((1+\zeta) U R_{G g,t}) + \lambda_{g,t}^{GD} ((1+\zeta) D R_{G g,t}) \right\} \right. \\
& \left. + \underline{\sigma} \lambda_{g,t}^{\Delta\sigma} + \underline{\sigma} \underline{\mu}_{g,t}^{\sigma} + \bar{\sigma} \bar{\mu}_{g,t}^{\sigma} \right\} + \sum_t \lambda_t^{\sigma} + \sum_{p,t} \bar{Q}_{Pp} (\bar{\mu}_{p,t}^{qp} - \underline{\mu}_{p,t}^{qp}) + \sum_{j \in (\Psi_W - \Psi_{W_s}),t} \left\{ \underline{Q}_{S j,t} \underline{\mu}_{j,t}^{qs} + \bar{Q}_{S j,t} \bar{\mu}_{j,t}^{qs} + \bar{Q}_{S j,t} \bar{\mu}_{j,t}^{rus} + \underline{Q}_{S j,t} \underline{\mu}_{j,t}^{rds} \right\}
\end{aligned} \tag{66}$$

4.2. Proposed Solution Method

As observed in Section 2, the problem of optimal participation of SEPs in the electricity market depends on the variables λ^{GE} , Q_S , $R U_S$, and $R D_S$, the amount of which can be calculated from the problem (49). Also, for the problem of optimal participation of SGPs in the gas market, the values of variables λ^{EE} , P_G , $R U_G$, and $R D_G$ should be obtained from (48). Therefore, the process of the proposed scheme corresponds to the decomposition solution technique. This paper uses the MSD method [23] to achieve the optimal solution to these problems in the shortest possible time. In this method, the KKT model of (48) is considered the master problem (MP), and the KKT model of

formulation (49) is solved in the slave problem (SP). Hence, the solution process is as follows [23]:

- *Step 1 (Initial MP)*: In this section, the initial values for the prices of gas energy and reserves markets, λ^{GE} , λ^{GU} , and λ^{GD} , and gas power and reserve of P2Gs, Q_S , $R U_S$, and $R D_S$, are taken into account. Then, the MP including the KKT model of (48) obtains optimal values for the price of electrical energy and reserve markets, $\hat{\lambda}^{EE}(v)$, $\hat{\lambda}^{EU}(v)$, and $\hat{\lambda}^{ED}(v)$, the active power and reserves of SEPs and non-SEPs, $\hat{P}_G(v)$, $R \hat{U}_G(v)$, and $R \hat{D}_G(v)$, where v is the iteration and is equal to 1 in this step. Also, the symbol “ $\hat{\cdot}$ ” represents the optimal value of a variable.

- *Step 2 (SP)*: This problem is formulated as follows:

The linear model of objective (27), i.e.(67) first term of Eq. (27) + right side of Eq.

$$(66) + \omega \cdot |x - \hat{x}|$$

Subject to:

Constraints (28)-(32) and KKT model(58) for the robust formulation of the problem (33)-(47) according to Eqs. (59)-(62)

This model is the same as the single-objective model for the problem (49), except that $\omega \cdot |x - \hat{x}|$ is added to the objective function. In this relation, x represents the variables λ^{EE} , λ^{EU} , λ^{ED} , P_G , RU_G , and, RD_G , and \hat{x} is the optimal value of these variables, which can be calculated from MP. Also, ω is a constant coefficient. It is possible that the SP problem will not be able to reach the optimal solution without the expression $\omega \cdot |x - \hat{x}|$ for \hat{x} values. To compensate it, the phrase $\omega \cdot |x - \hat{x}|$ is added

$$\max \left(\left| \tilde{x}(v) - \hat{x}(v) \right|, \left| \tilde{w}(v) - \tilde{w}(v-1) \right| \quad \forall b, g, i, j, t \right) \leq \varepsilon \quad (69)$$

$$\forall x = [P_G \quad RU_G \quad RD_G \quad \lambda^{EE} \quad \lambda^{EU} \quad \lambda^{ED}],$$

$$w = [Q_S \quad RU_S \quad RD_S \quad \lambda^{GE} \quad \lambda^{GU} \quad \lambda^{GD}]$$

where, ε is the permissible computational error or tolerance of the MSD method. It must be said that if the relation is not established, Step 4 must be performed, and v tends to $v + 1$.

- *Step 4 (MP)*: This problem is formulated as follows:

Linear model of objective (1), i.e. first(70) term of Eq. (1) + right side of Eq. (65) + $\omega \cdot |w - \tilde{w}(v-1)|$

Subject to:

Constraints (2)-(10) and KKT model for(71) robust formulation of problem (11)-(26)

to the upper-level objective function of the SGPs optimal participation problem. Therefore, in this case, the determined value of x in this step is equal to the optimal values of λ^{EE} , λ^{EU} , λ^{ED} , P_G , RU_G , and, RD_G in iteration v . Also, note that the expression $\omega \cdot |x - \hat{x}|$ is nonlinear. To linearize it, the term $\omega \cdot |x - \hat{x}|$ is replaced with $\omega \cdot (x^+ + x^-)$ in (67), where x^+ and x^- are auxiliary variables whose values following the constraints $x^+ + x^- = x - \hat{x}$, $0 \leq x^+ \leq M \cdot z$, and $0 \leq x^- \leq M \cdot (1 - z)$ are determined by problem (67)-(68). Also, M is a large fixed number and z is an auxiliary binary variable. Finally, the optimal values of the variables calculated in this step are denoted by the symbol “ \sim ”.

- *Step 3 (Convergence analysis)*: The problems proposed in Section 2 meet the convergence conditions if the following equation is established:

according to Eqs. (59)-(62)

The above problem has the same framework as the SP problem, except that this problem is according to single-objective model for formulation (48). Also, the linearization process of $\omega \cdot |w - \tilde{w}(v-1)|$ is the same as that of $\omega \cdot |x - \hat{x}|$. Finally, the results of this step are applied to the second step and the problem solving is repeated from the second step.

5. NUMERICAL RESULTS

5.1. Case Study 1

A) *Problem data:* In this section, the proposed scheme is applied to the test system presented in Fig. 2, which has a standard IEEE 6-bus transmission network with a base power of 100 MW, and a 7-node gas network with a base gas amount of 1000 Sm³. Characteristics of transmission lines, pipelines, and P2Gs are provided in [24]. As it is seen in Fig. 2, the gas system includes 6 GW, the specifications of which are described in [24], and their operation prices are 0.9, 0.8, 0.6, 0.6, 0.7, and 0.5 \$/Sm³, respectively. GWs in nodes 1-3 is non-SGP, however, others GWs are SGP. The characteristics of the generation units are also listed in Table 2. In addition, the electrical network has a peak load of 763 MW, which

is divided between buses 3 to 6 to about 19%, 27%, 27%, and 27%, respectively [16]. The peak gas load is equal to 6800 Sm³ which is divided into nodes 2, 4, and 6 by about 50%, 33%, and 17%, respectively [16]. Also, the daily electric and gas load curves for the mentioned networks are proportional to the product of the power rate curve in Fig. 3(a) [16] and the peak load. In addition, it is assumed that the FRU in this paper has a wind farm whose position, wind system capacity, and ESS characteristics are presented in Table 2, but the daily wind system power rate curve is provided in Fig. 3(a) [25]. In other words, the active power produced by the wind farm per hour is equal to the product of the capacity of the wind system and the rate of power at that hour.

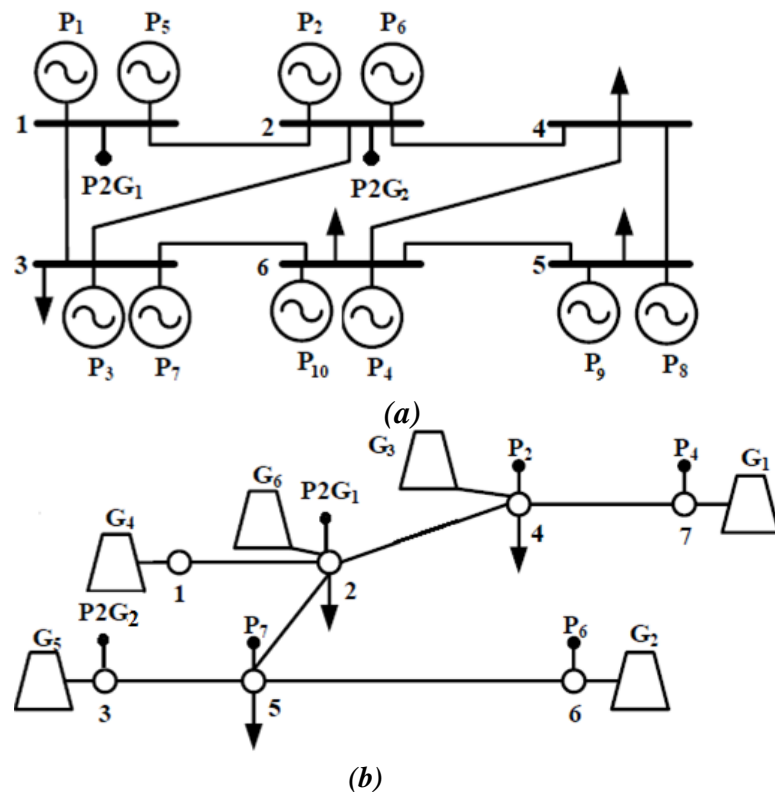


Fig. 2. The test system under study, a) the IEEE 6-bus transmission network, and b) 7-node gas network [24].

Table 2. Data of generation units [24].

Unit	Type	SEP	Electric bus	Gas node	$\bar{P}_G / \underline{P}_G$ (MW)	Fuel price (\$/MWh)	Efficiency (%)
1	Coal	Yes	1	-	155/0	10.5	-
2	GFU	Yes	2	4	90/0	-	52
3	Coal	Yes	3	-	155/0	10.5	-
4	GFU	Yes	6	7	197/0	-	54
5	Coal	No	1	-	320/0	20.7	-
6	GFU	No	2	6	197/0	-	55
7	GFU	No	3	5	197/0	-	51
8	Coal	No	5	-	155/0	10.5	-
9	FRU	Yes	5	-	40*/5#/5**/30##	0	-
10	FRU	Yes	6	-	40*/5#/5**/30##	0	-

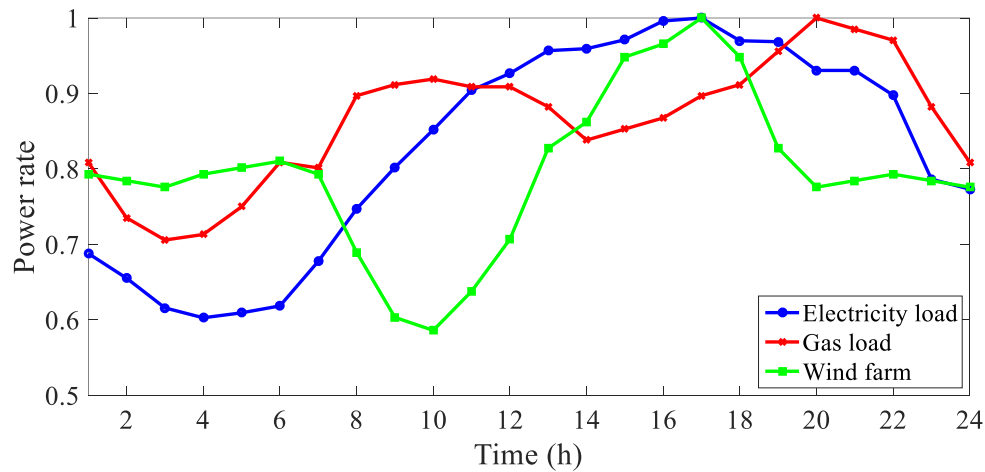
* Wind farm capacity (MW), # Charge/discharge rate of ESS (MW), ** Minimum energy of ESS (MWh), ## Maximum energy of ESS (MWh)

The current study assumes that the bus/node to which a generation unit/gas producer is connected can have reserve services. Therefore, according to Fig. 2, buses 1, 2, 3, 5, and 6 have reserve equipment, where the daily curve of up and down reserve demand for each bus is shown in Fig. 3(b) [26]. Also, there are gas producer in nodes 1-4 and 6-7, so these nodes have reserve services, the daily curve of up and down reserve demand for each node is as in Fig. 3(b). Finally, the proposed problem is coded in the GAMS software environment, and then the CPLEX solver [27] is used to achieve the optimal solution to the master-slave problems. Moreover, the permissible computational error and computational tolerance, ε , for the MSD algorithm in this paper are set at 0.01.

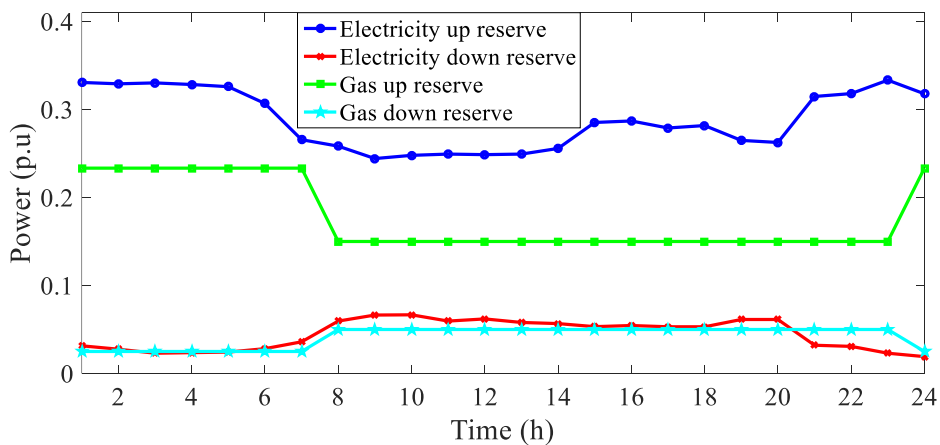
B) *Evaluation of the convergence curve of the MSD algorithm for the proposed scheme*: The process of solving the proposed problem using the MSD method was presented in Section 4.2. The convergence results of this solver for the deterministic model of the problem ($\zeta = 0$) and its robust model ($\zeta = 0.1$ and $\zeta = 0.2$) are shown in Fig. 4. Based on this, it can be seen that in the deterministic model, the mentioned algorithm has reached the convergence point with a computational tolerance of 0.01 in 7 iterations and 40.2 seconds. However, in robust models with $\zeta = 0.1$ and $\zeta = 0.2$, the convergence iterations are 8 and 9, respectively, which correspond to the computational times of 50.6 and 61.3 seconds, respectively. It is noteworthy that the increase in the number of convergence iterations or computational time in case of

increasing the level of uncertainty according to Section 3 is due to the reduction in the feasibility region of the problem in the worst case scenario compared to the scenario corresponding to the deterministic model ($\zeta = 0$). Therefore, the optimal solution can be achieved with a longer computational time. In addition, as shown in Fig. (4), in all the models studied for the proposed scheme in

this section, the MSD algorithm approaches the convergence point at fewer iterations. So that in 4 iterations, the calculation error for all levels of presented uncertainty is less than 0.5. Thus, it can be stated that the algorithm used in this section has the desired ability to achieve the optimal solution in fewer iterations and shorter convergence time.



(a)



(b)

Fig. 3. Daily curve, a) power rates electric load, gas load, and wind farm [25], b) up and down reserve demands [26] in transmission network buses and gas network nodes.

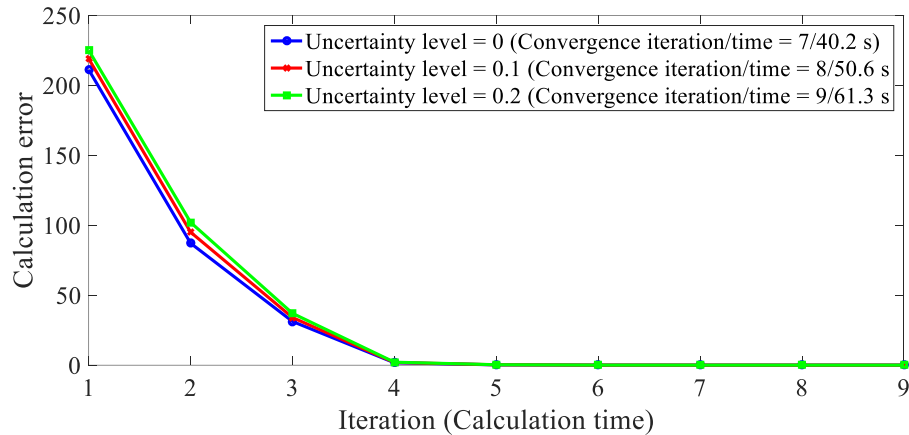


Fig. 4. Convergence curve of the MSD method for different uncertainty levels in the proposed robust model.

C) *Investigating the participation of SEPs in the coupled electricity and gas market:* The results of this section are presented in Figs. 5 to 7 and Table 3. Fig. 5 shows the daily injection active power curve of generation units in the transmission network for different values of the uncertainty level. Based on this figure, it can be seen that generation units with NGFU type inject more power into the grid, or feed a high percentage of the electrical load than other units at all simulation hours. By comparing the performance of NGFU with GFU it can be stated that the fuel price stated in Table 2 is for the active power generation of NGFU, where units 1, 3, and 8 have the lowest fuel price, i.e., 10 \$/MWh ($10.5 \text{ (\$/MWh)} * 100 \text{ (MW)} = 1050 \text{ (\$/p.u)}$). However, the fuel price of GFU for its input gas is listed in Section 5.1(a). Therefore, its efficiency also impacts the operation of the GFU. Since the efficiency of GFUs according to Table 1 is around 50%, and the fuel price of GWs is more than 0.5 \$/Sm³ ($0.5 \text{ (\$/Sm}^3) * 1000 \text{ (Sm}^3) = 500 \text{ (\$/p.u)}$), It can be stated that the fuel price for electrical power generation in GFUs is more than 1050 \$/p.u. Therefore, to

minimize the operation cost of generation units, it is expected to use units with lower fuel costs, which according to Table 1 are equal to NGFUs 1, 3 and 5, and FRUs 9 and 10. Therefore, the amount of active power generation of NGFUs in Fig. 5(a) will be more than that of GFUs in Fig. 5(b). By comparing the performance of NGFU and FRU in this case study, it can be said that the total capacity of NGFUs according to Table 1 is much higher than that of FRUs; hence, the generation output of NGFUs in Fig. 5(a) is much higher than that of FRUs in Fig. 5(c).

The trend of changes of active power for NGFUs and GFUs based on Figs. 5(a) and (b) and Fig. 3(a) is close to that of electric load, but this is not the case for FRUs because NGFUs and GFUs are only responsible for supplying the electrical network load. Yet, FRUs, in addition to supplying the transmission network, must also charge their internal batteries to be prepared for critical hours, such as peak load times. Therefore, according to Fig. 5(c), they perform charging operations from 1:00 to 9:00 and 23:00 to 24:00, which corresponds to the off-peak hours according to Fig. 3(a) and perform

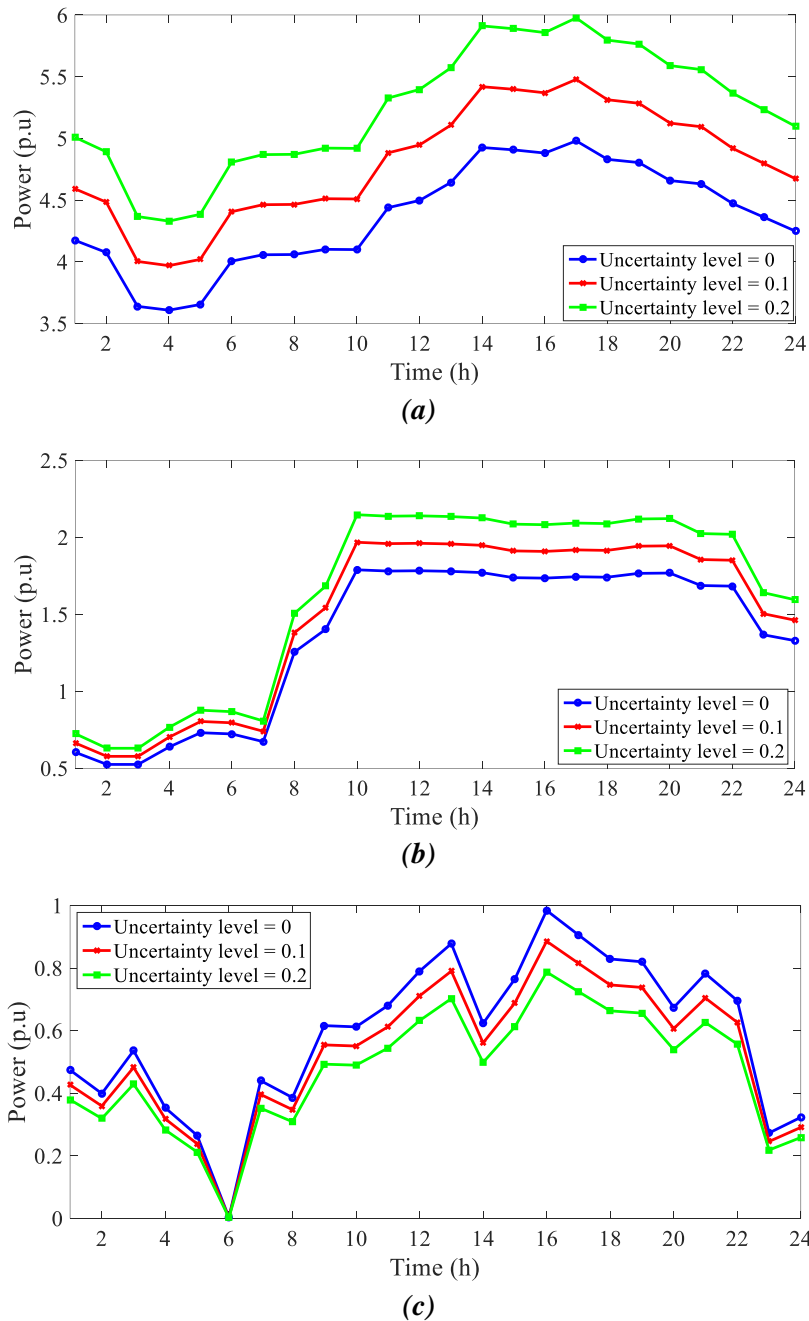


Fig. 5. Daily power curve, a) NGFUs, b) GFUs, c) FRUs for different uncertainty levels in the proposed robust model.

discharging operations during other hours because, according to Table 2 and Fig. 3(a), it can be said that the total capacity of wind farms in FRUs for 1:00 to 9:00 and 23:00 to 24:00 is about 0.7 p.u. While in Fig. 5(c), the generation power of FRUs is less than this

number. This means that part of generation power of the wind farm is consumed inside the FRUs, which means that the internal ESSs of the FRUs are charged. The opposite is true at other hours, i.e., when the generation power of FRUs in Fig. 5(c) is

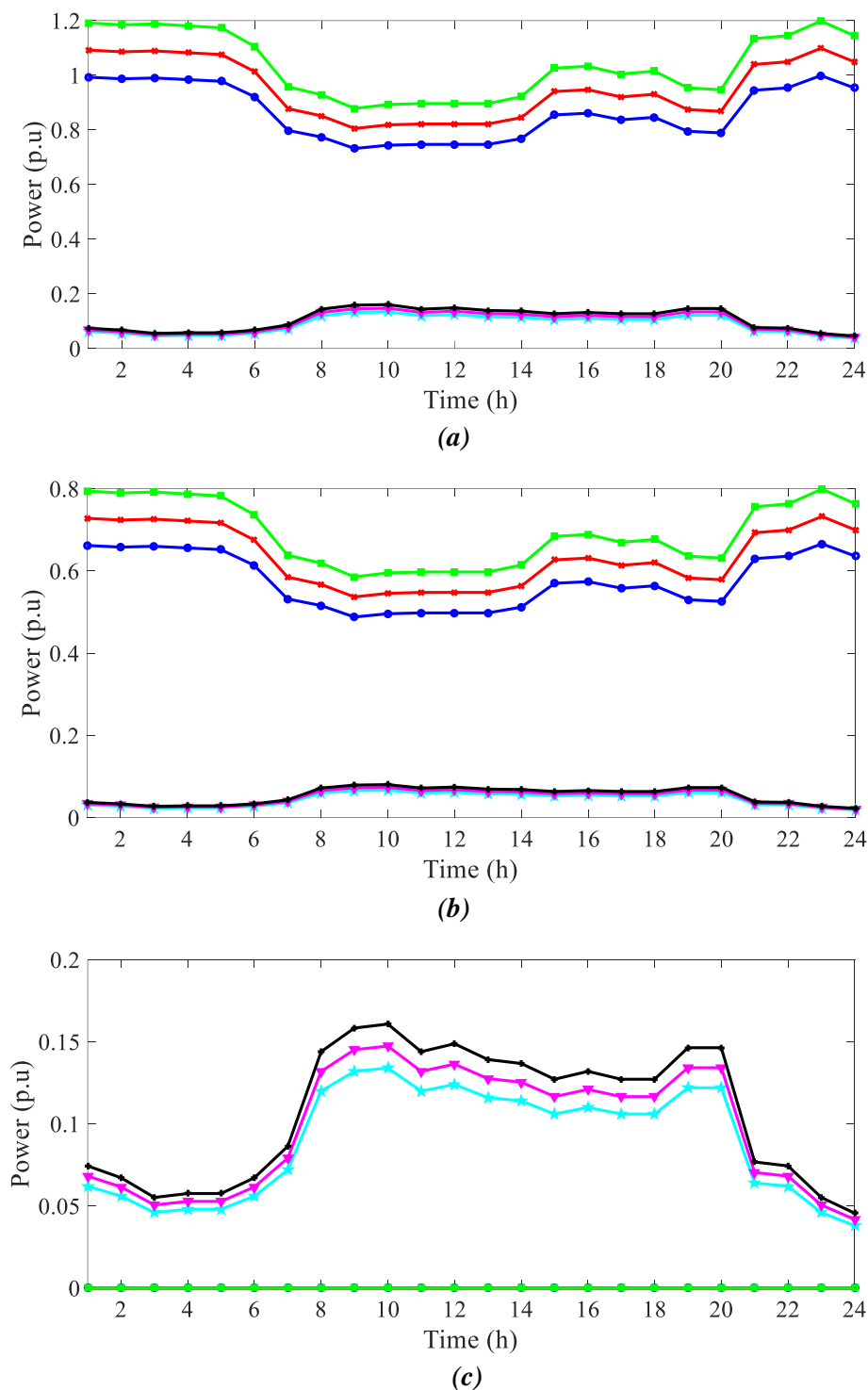


Fig. 6. Daily up/down reserve curve, a) NGFUs, b) GFUs, and c) FRUs for different uncertainty levels.

greater than that of wind farms based on Fig. 3(a). Thus, ESSs inject power into the grid during these hours, so the generation output

of FRUs will be more than wind farms. Finally, it should be noted that increasing the uncertainty level reduces the generation

output of FRUs, which is due to reducing the generation output of wind farms based on (48) in the worst-case scenario. However, the generation outputs of GFUs and NGFUs increase in these conditions because the amount of transmission network load increases with ζ based on (48). Since a high percentage of electrical loads is provided by GFUs and NGFUs according to Fig. 5, their generation power will increase with increasing the uncertainty level.

Fig. 6 illustrates daily reserve power curve of generation units in the transmission network for deterministic ($\zeta = 0$) and robust ($\zeta = 0.1$ and $\zeta = 0.2$) models. In this section, units with NGFU have more participation in

the mentioned market than other electricity producers. This is also due to their low fuel cost compared to GFUs, and their high capacity compared to FRUs. In addition, increasing the uncertainty level in the robust model compared to the deterministic model increases the level of reserve generated by all generation units because the reserve demand in these conditions in the worst-case scenario based on (48) is more than the scenario corresponding to the deterministic model. Thus, since the reserve demand supplier in different buses is realized by NGFUs, GFUs, and FRUs, it is expected that the generation reserve power of these units will increase with increasing ζ .

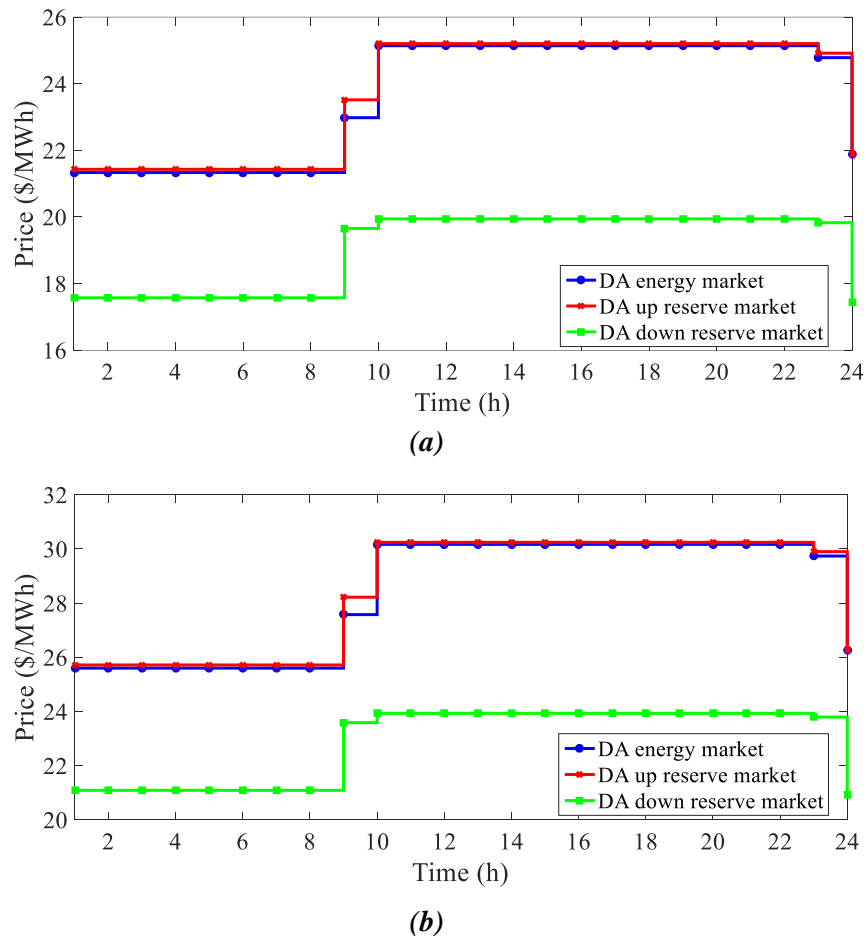


Fig. 7 Daily average price curve for energy/up reserve/down reserve markets in the robust model with, *a*) uncertainty level between 0-0.3, and *b*) uncertainty level between 0.3-0.5.

The daily average price curve for energy, up and down reserve markets for the uncertainty levels of 0 to 0.5 is shown in Fig. 7. Based on this figure, it can be observed that the energy price has two levels: at the lower level corresponding to the hours from 1:00 to 8:00, the price is around 21.5 \$/MWh (2150 \$/p.u) to 25.8 \$/MWh (2580 \$/p.u) for uncertainty level between 0-0.3 and 0.3-0.5, respectively. At the high level corresponding to 9:00 to 24:00, for uncertainty level between 0-0.3 and 0.3-0.5, the price is around 25 \$/MWh (2500 \$/p.u) and 30.5 \$/MWh (3050 \$/p.u). It should be noted that according to [28], the market price depends on the fuel price of generation units, transmission line congestion, and network losses. Since the DC power flow model, Eqs. (12)-(14), has been used for the proposed scheme, the network losses are zero and its effect on the market price is neglected in this study. Also, if there is no line congestion, the market price should be less than the maximum fuel price. Nonetheless, since according to Table 2 the highest fuel price belongs to NGFU 5, i.e., 20.7 \$/MWh, the congestion of the transmission lines has resulted in the energy price at all simulation hours exceeding 20.7 \$/MWh. From 9:00 to 24:00, the amount of load is more than that from 1:00 to 8:00, so the number of congested transmission lines in the hours from 9:00 to 24:00 compared to the period from 1:00 to 8:00 is higher. Therefore, the energy price from 9:00 to 24:00 will be higher than that from 1:00 to 8:00. In addition, according to Section 5.1.A, as the power level demand by the up reserve is high at all simulation hours, and the amount of active power consumed is also high,

generation units with higher fuel prices participate in supplying the up reserve demand. Hence, the price in the DA up reserve market will be close to the energy price at all simulation hours. Nonetheless, the demand level of down reserve is low based on Fig. 3(b), so it is supplied by electricity producers with low fuel prices. Hence, the price in the DA down reserve market is much lower than the energy price in all simulation hours. In addition, increasing the uncertainty level will increase the electrical load and the demand for up and down electrical reserves and reduce the generation output level of wind farms based on (48). This will, therefore, increase the price in the mentioned markets compared to the deterministic model because, in this case, the number of congested transmission lines will increase and generation units with higher fuel prices will be utilized for energy supply and reserve. Finally, according to the topics presented in this section, the cost, revenue, and profit of SEPs at different uncertainty levels will correspond to the results presented in Table 3. Accordingly, the operation cost of SEPs increases by increasing ζ because, according to Fig. 5, the generation output of NGFUs and GFUs has increased under these conditions, but the output of FRUs has decreased. The

Table 3. Economic results of SEP for different uncertainty levels in the proposed robust model.

Index	$\zeta = 0$	$\zeta = 0.1$	$\zeta = 0.2$
Cost (\$)	208450	231380	252224
Revenue (\$)	438940	452108	456450
Profit (\$)	230490	220728	204226

same is true for SEPs revenue, except that the percentage increase in revenue is lower than the cost. Thus, with an increase in ζ , the profit of SEPs decreases.

D) *Participation of SGPs in the coupled electricity and gas market*: Fig. 8 depicts the daily curve of the amount of gas provided by gas producers in the gas network in the energy, up and down reserve services for different uncertainty levels. Accordingly, GW provides the energy required for the gas network and GFUs and the reserve demand for this network. In other words, P2Gs are always switched off because the operation cost of the gas they produce at their own output depends on the price of electricity and their own efficiency. As shown in Fig. 7, the average price of electrical energy is more than 20 \$/MWh (2000 \$/p.u), and the efficiency of P2Gs is about 50% based on [24]. Therefore, the operation price for P2G's output gas is more than 4000 \$/p.u (2000/0.5), which is much higher than the highest operation price of GW, i.e. 0.9 \$/Sm³ (900 \$/p.u) for GW 1 according to Section 5.1.A. Therefore, the proposed scheme does not use P2Gs due to their high operation costs, provided that the GW capacity meets the demand for grid gas and GFUs. As a result, they are utilized only in critical situations where the demand for gas network consumption exceeds the generation capacity of GW. In addition, it can be seen from Fig. 8 that an increase of ζ in the robust model compared to the deterministic model ($\zeta = 0$) increases the gas produced by GWs in the energy and reserves services as, based on (49), the demand for load and reserve in the gas network increases under these conditions. Also, the amount of gas demand by the GFUs

increases according to Figs. 5 and 6 by increasing ζ .

Fig. 9 shows the daily price curve in the DA energy, up and down reserve gas markets for the uncertainty level between 0 and 0.5. Based on Fig. 9, the price in the DA down gas reserve market is fixed for all simulation hours, but the price in the DA gas energy and up reserve markets has two levels, high and low. The low level occurs at 1:00 to 8:00, which corresponds to the low load in the electrical and gas network according to Fig. 3(a). However, the high level is proportional to the peak hours of the electrical and gas network according to Fig. 3(a), which occurs between 9:00 and 24:00. Referring to Fig. 9, the price of up and down gas reserve markets is higher than the price of gas energy market, which means that GWs with high operation prices participate in the provision of gas reserves. For example, to provide a gas reserve in node 7, the use of GW 1 is required, the operation price of which is 0.9 \$/Sm³. Yet, gas energy can be supplied by GWs with low operation costs, which is due to the consideration of the energy transfer model from one node to another. Therefore, the price in the gas reserve market will be higher than that in the gas energy market. Furthermore, the price increase in different markets in terms of increasing the uncertainty level of 0.3 is stepwise as in Fig. 7. This indicates that at an uncertainty level of less than 0.3, increased gas demand in various markets can be met by cheaper GW. Also, by increasing the uncertainty level to greater than 0.3, more expensive GWs like GW 1 will be switched on. Thus, the market price will change in steps. Finally, according to Figs. 8 and 9, the amount of economic indices

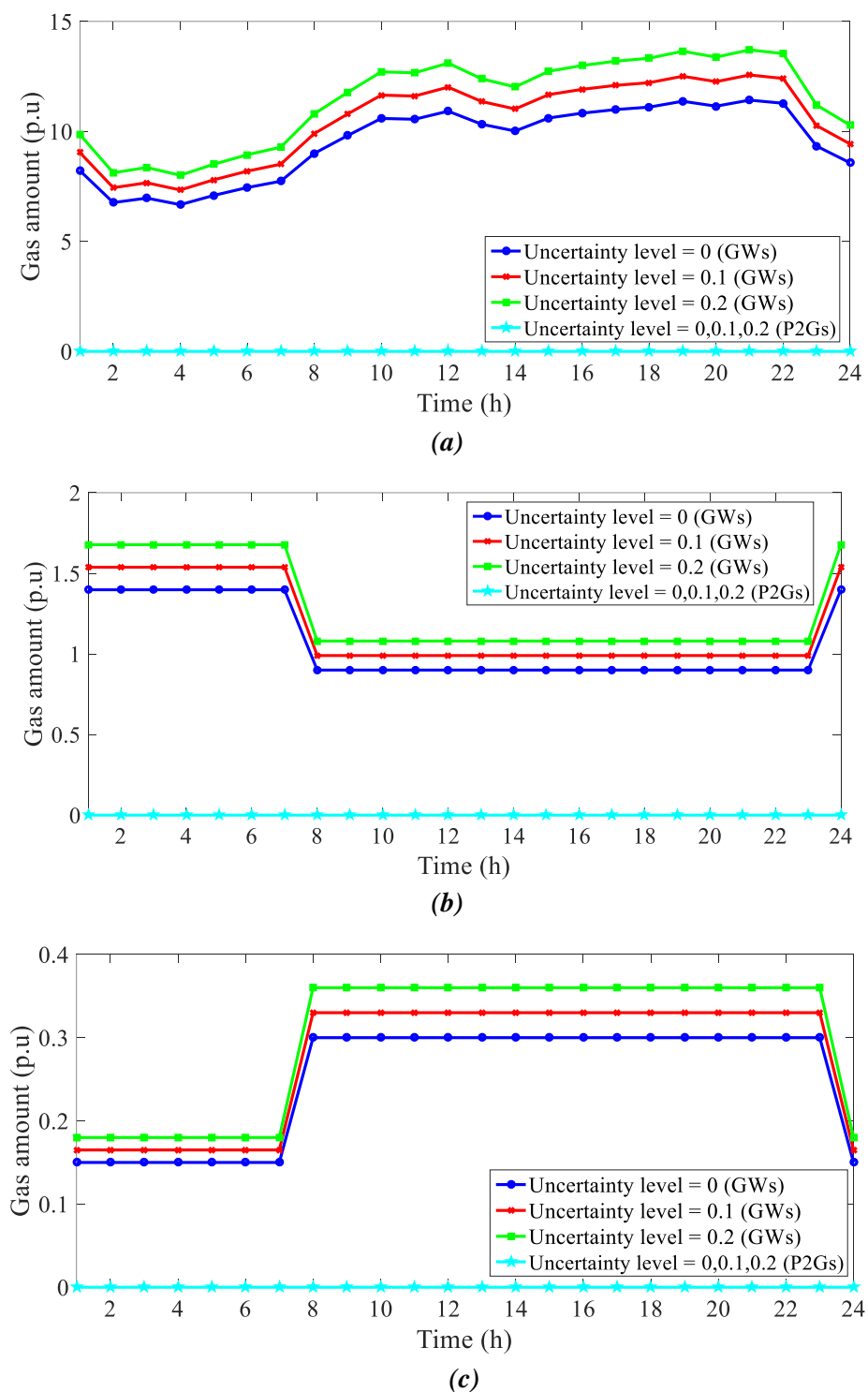


Fig. 8. Daily curve of GWs in a) energy service, b) up reserve service, and c) down reserve service for different uncertainty levels in the proposed robust model.

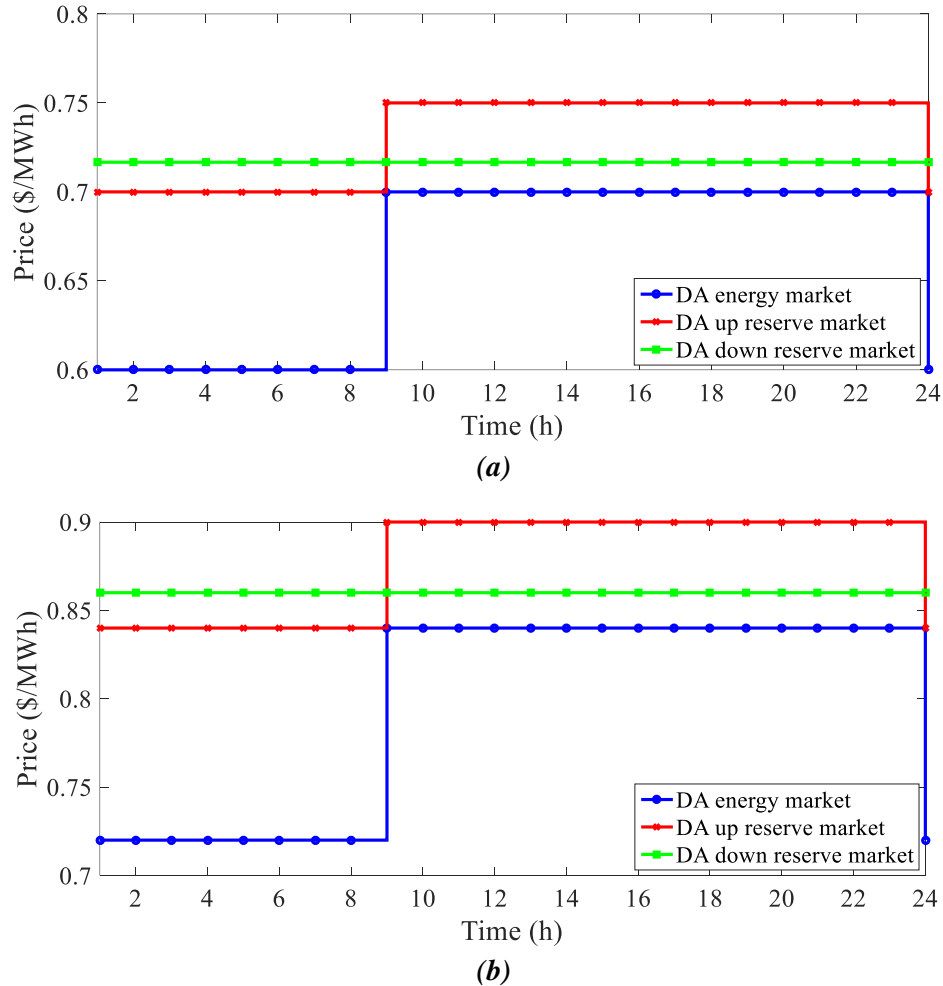


Fig. 9. Daily average price curve of energy/up reserve/down reserve markets in the robust model with, *a)* uncertainty level between 0-0.3, *b)* uncertainty level between 0.3-0.5.

Table 4. Economic results of SGPs for different uncertainty levels in the proposed robust model.

Index	$\zeta = 0$	$\zeta = 0.1$	$\zeta = 0.2$
Cost (\$)	155240	170764	186288
Revenue (\$)	186390	193846	197573
Profit (\$)	31150	23082	11285

of SGPs will correspond to Table 4. By comparing Tables 2 and 3, one can observe that the revenue of SEPs will be much higher than that of SGPs, which can be due to the

higher price of energy and reserves in the electricity market compared to the gas market (refer to Figs. 7 and 9). Hence, the profit of SEPs is much higher than that of SGPs. As the results of Table 3 state, increasing the uncertainty level in the robust model compared to the deterministic model of the proposed scheme increases the cost and revenue of SGPs. This is because of the increase in gas demand in the energy and reserve market. However, the increasing percentage in revenue is less than the cost, so an increase of ζ reduces the profit of SGPs.

Table 5. Characteristics of generation units in the IEEE 24-bus transmission network.

Unit	Type	SEP	Electric bus	Gas node	$\bar{P}_G / \underline{P}_G$ (MW)	Fuel price (\$/MWh)	Efficiency (%)
1	Coal	Yes	1	-	192/0	10.5	-
2	Coal	Yes	2	-	192/0	10.5	-
3	Coal	No	7	-	300/0	15.2	-
4	GFU	Yes	13	2	300/0	-	50
5	Coal	Yes	14	-	100/0	8.6	-
6	GFU	No	15	7	205/0	-	54
7	GFU	Yes	16	6	100/0	-	50
8	GFU	Yes	18	1	100/0	-	53
9	Coal	No	21	-	100/0	8.6	-
10	GFU	Yes	22	4	600/0	-	55
11	Coal	Yes	23	-	300/0	15.2	-
12	FRU	Yes	14	-	40*/5#/5**/30##	0	-
13	FRU	Yes	16	-	40*/5#/5**/30##	0	-
14	FRU	Yes	18	-	40*/5#/5**/30##	0	-
15	FRU	No	21	-	40*/5#/5**/30##	0	-

*Wind farm capacity (MW), # Charge/discharge rate of ESS (MW), ** Minimum energy of ESS (MWh), ## Maximum energy of ESS (MWh).

5.2. Case Study 2

In this section, the problem data is the same as in Section 5.1.A, except that in this section, the IEEE 24-bus network is selected as the electrical system. The characteristics of transmission lines and electrical load are presented in [29]. The data corresponding to generation units is also listed in Table 5. In addition, as stated in Section 5.1.A, reserve services are assumed to be available on buses with electricity producer. Therefore, according to Table 5, buses 1, 2, 7, 13-16, 18,

and 21-23 provide this service; the corresponding data for each mentioned bus is shown in Fig. 3(c). Also, in this network, FRUs include a wind farm whose daily power rate curve is as Fig. 3(b). It is assumed that two P2Gs in the gas network are able to purchase active power from buses 7 and 14.

The results of this section are presented in Table 6. Based on this table, it can be seen that in the worst-case scenario, assuming the uncertainty level of 0.2, the MSD algorithm was able to achieve the optimal solution in 23 iterations and a computational time of 145.1

Table 6. The results of the coupled electricity and gas market in Case study 2.

Convergence of the proposed solution method						
Uncertainty level	Convergence iteration	Computational time (second)		Calculation error (p.u)		
0	13	72.4		0.01		
0.1	17	104.6		0.01		
0.2	23	145.1		0.01		
Economic results						
Uncertainty level	SEPs			SGPs		
	Cost (\$)	Revenue (\$)	Profit (\$)	Cost (\$)	Revenue (\$)	Profit (\$)
0	394210	541730	147530	161220	198150	36930
0.1	433631	563400	129769	177342	204095	26753
0.2	473052	573651	100599	193464	208057	14593

seconds by accepting an allowable error tolerance of 0.01. The lower the uncertainty level, the better the situation. It can also be seen, as stated in Section 5.1, that an increase in ζ increases the cost and revenue of SEPs and SGPs, so that the rate of revenue increase is less than that of the cost. Therefore, an increase of ζ in the robust model compared to the deterministic model will reduce the profit for SEPs compared to SGPs. Thus, in the worst-case scenario with an uncertainty level of 0.2, the total profit of SEPs compared to SGPs in comparison with that of the deterministic model will be about 69268\$ (147530 + 36930 - 100599 - 14593) for case study 2.

6. CONCLUSIONS

This paper presents the participation of SEPs and SGPs in the DA coupled electricity and gas market with energy and reserve services

corresponding to the EMS model. In this scheme, two bi-level problems were presented, each of which referred to the participation of SEPs or SGPs in the DA energy and reserve markets based on the MCP model. In these problems, the upper-level model has an objective function aiming to minimize the difference between the cost and revenue of SEPs or SGPs in the mentioned markets constrained to these producers' operation model. Also, in the lower-level formulation, the MCP model was presented, which minimizes the operation costs of non-SEPs or non-SGPs constrained to the electrical or gas network model in the presence of electricity or gas producers. In addition, a robust programming was used to model uncertainties of the load, reserve demand, and generation power of wind farms. Then, the MSD algorithm was exploited to achieve the optimal solution in

this study. Finally, based on the numerical results, it was proved that the proposed algorithm is also applicable to larger networks, which can obtain the optimal solution with the least computational error in the shortest possible computational time. The proposed scheme generally uses electricity and gas producers with low operation costs to increase social welfare for energy and reserve supply. It also uses more expensive units such as P2Gs in critical situations where energy consumption and reserves exceed the generation output of units with low operation costs. Besides, the suggested scheme was able to achieve significant profits for SEPs or SGPs even in the worst-case scenario by implementing an appropriate management system in electrical and gas networks. Note that, this paper assumes that the market operator is in communication and coordination with the electricity and gas network operator. Therefore, in these conditions, the mentioned market is applicable. In addition, the results of this paper can be an incentive for producers and operators of electricity and gas networks and encourage them to participate in the coupled electricity and gas market.

NOMENCLATURE

1) Indices and Sets

b, Ψ_B	Indices and set of electrical buses
g, Ψ_N	Indices and set of gas nodes
i, Ψ_G, Ψ_G^{FR}	Indices and set of generation units,
Ψ_G^{G2P}, Ψ_{G_s}	set of flexi-renewable unit (FRU),
$\Psi_{G_s}^{FR}$	set of gas-fired unit (GFU), set of

		SEPs, and set of SEP with type of FRU
$j, \Psi_W, \Psi_W^{P2G}, \Psi_{W_s}$		Indices and set of gas well (GW), set of power to gas (P2G), and set of SGPs
k, Ψ_K		Indices and set of linearization segments for gas pressure term
l, Ψ_L		Indices and set of transmission lines
p, Ψ_P		Indices and set of gas pipelines
s, Ψ_S		Indices and set of scenario samples
t, Ψ_T		Indices and set of simulation hours

2) Variables

P_C, P_D	Active charging/discharging power of the energy storage system (ESS) in per unit (p.u)
P_G, RU_G, RD_G	Active, up and down reserve power of generation unit (p.u)
P_L	Active power flowing from transmission line (p.u)
Q_S, RU_S, RD_S	Gas amount of gas producer in energy, up and down reserve markets (p.u)
Q_P	Gas amount flowing from pipeline (p.u)
δ	Voltage angle (rad)
λ, μ	Lagrangian multipliers

λ^{EE} ,	Local electricity marginal price (LEMP)	\underline{E}, \bar{E}	Minimum and maximum energy of the
λ^{EU} ,	for energy, up and down reserve markets		ESS (p.u)
λ^{ED}	(\$/MWh)	F	Incidence matrix of electrical buses and
λ^{GE} ,	Local gas marginal price (LGMP) for		P2G
λ^{GU} ,	energy, up and down reserve markets	H	Incidence matrix of gas nodes and
λ^{GD}	(\$/Sm ³)		pipelines
$\sigma, \Delta\sigma$	Magnitude and deviation of gas pressure	m^σ, m^γ	Slopes of linearization segments of σ
	(p.u)		and $\Delta\gamma$
$\Delta\gamma$	Auxiliary variable (p.u)	P_D	Active load (p.u)
3) Constants:			
A	Incidence matrix of electrical buses and	$\underline{P}_G, \bar{P}_G$	Minimum and maximum active power of
	generation unit		the generation unit (p.u)
B	Incidence matrix of gas nodes and	\bar{P}_L	Maximum capacity of transmission lines
	generation unit		(p.u)
B_L	Susceptance of the transmission line	P_W	Active power of the wind farm (p.u)
	(p.u)	Q_D	Gas load (p.u)
C	Incidence matrix of electrical buses and	\bar{Q}_P	Maximum capacity of pipelines (p.u)
	transmission lines considering current	$\underline{Q}_S, \bar{Q}_S$	Minimum and maximum power of gas
	direction		producer (p.u)
CR, DR	Charging and discharging rates of the	UR_E	Up reserve demand in electrical buses
	ESS (p.u)		(p.u)
D	Incidence matrix of gas nodes and gas	UR_G	Up reserve demand in gas nodes (p.u)
	producer	α	Operation price of gas wells (\$/Sm ³)
DR_E	Down reserve demand in electrical buses	β	Fuel cost of non-GFU (\$/MWh)
	(p.u)	π	Probability of occurrence
DR_G	Down reserve demand in gas nodes (p.u)	η	Efficiency of GFU and P2G
$E(0)$	Initial energy of the ESS (p.u)	η_C, η_D	Charging and discharging efficiency of
			the ESS (p.u)

κ Pipeline constant (p.u)

REFERENCES

- [1] K. Afrashi, B. Bahmani-Firouzi, M. Nafar, "IGDT-Based Robust Optimization for Multicarrier Energy System Management," *Iranian Journal of Science and Technology, Transactions of Electrical Engineering*, (accepted), 2020.
- [2] J. Fan, X. Tong, "Optimal Location Allocation Strategy of Gas-fired Unit in Transmission Network," *Journal of Modern Power Systems and Clean Energy*, vol. 8, pp. 229-237, 2020.
- [3] M. Gökçek, C. Kale, "Techno-economical evaluation of a hydrogen refuelling station powered by Wind-PV hybrid power system: A case study for İzmir-Çeşme," *International Journal of Hydrogen Energy*, vol. 43, pp. 19615-10625, 2018.
- [4] H.R. Zafarani, S.A. Taher, M. Shahidehpour, "Robust operation of a multicarrier energy system considering EVs and CHP units," *Energy*, vol. 192, pp.1-12, 2020.
- [5] K. Afrashi, B. Bahmani-Firouzi, M. Nafar, "Multicarrier Energy System Management as Mixed Integer Linear Programming," *Iranian Journal of Science and Technology, Transactions of Electrical Engineering*, (accepted), 2020.
- [6] Y. Cao, et al., "Optimal operation of CCHP and renewable generation-based energy hub considering environmental perspective: An epsilon constraint and fuzzy methods," *Sustainable Energy, Grids and Networks*, vol. 20, pp. 100274, 2019.
- [7] A.A. Eladl, et. al., "Optimal operation of energy hubs integrated with renewable energy sources and storage devices considering CO2 emissions," *International Journal of Electrical Power & Energy Systems*, vol. 117, pp. 105719, 2020.
- [8] X. Lu, Z. Liu, L. Ma, L. Wang, K. Zhou, S. Yang, "A robust optimization approach for coordinated operation of multiple energy hubs," *Energy*, vol. 197, pp. 117171, 2020.
- [9] A. Mirzapour-Kamanaj, M. Majidi, K. Zare, R. Kazemzadeh, "Optimal strategic coordination of distribution networks and interconnected energy hubs: A linear multi-follower bi-level optimization model," *International Journal of Electrical Power & Energy Systems*, vol. 119, pp. 105925, 2020.
- [10] F. Jamalzadeh, A. Hajiseyed-Mirzahosseini, F. Faghihi, M. Panahi, "Optimal operation of energy hub system using hybrid stochastic-interval optimization approach," *Sustainable Cities and Society*, vol. 54, pp.101998, 2020.
- [11] A. Dini, S. Pirouzi, M.A. Norouzi, M. Lehtonen, "Grid-connected energy hubs in the coordinated multi-energy management based on day-ahead market framework," *Energy*, vol. 188, pp. 116055, 2019.
- [12] J. Aghaei, M. Barani, M. Shafie-khah, A. A. Sánchez de la Nieta and J. P. S. Catalão, "Risk-Constrained Offering Strategy for Aggregated Hybrid Power Plant Including Wind Power Producer

- and Demand Response Provider,” IEEE Transactions on Sustainable Energy, vol. 7, no. 2, pp. 513-525, April 2016.
- [13] A. Jamali et al., “Self-Scheduling Approach to Coordinating Wind Power Producers With Energy Storage and Demand Response,” IEEE Transactions on Sustainable Energy, vol. 11, no. 3, pp. 1210-1219, July 2020.
- [14] X. Xu, W. Hu, D. Cao, Q. Huang, W. Liu, C. Chen, H. Lund, Z. Chen, “Economic feasibility of a wind-battery system in the electricity market with the fluctuation penalty,” Journal of Cleaner Production, vol. 271, pp. 122513, 2020.
- [15] M. Hamwi, I. Lizarralde, J. Legardeur, “Demand response business model canvas: A tool for flexibility creation in the electricity markets,” Journal of Cleaner Production, vol. 282, pp. 124539, 2020.
- [16] C. Wang, W. Wei, J. Wang, F. Liu and S. Mei, “Strategic Offering and Equilibrium in Coupled Gas and Electricity Markets,” IEEE Transactions on Power Systems, vol. 33, no. 1, pp. 290-306, Jan. 2018.
- [17] N. Padmanabhan, et.al., “Battery Energy Storage Systems in Energy and Reserve Markets,” IEEE Transactions on Power Systems, vol. 35, pp. 215-226, 2020.
- [18] S.A. Bozorgavari, et.al., “Two-stage hybrid stochastic/robust optimal coordination of distributed battery storage planning and flexible energy management in smart distribution network,” Journal of Energy Storage, vol. 26, pp. 100970, 2019.
- [19] H. Hamidpour, et.al., “Integrated resource expansion planning of wind integrated power systems considering demand response programmes,” IET Renewable Power Generation, vol. 13, no. 4, pp. 519-529, 18 3 2019.
- [20] J. Aghaei, N. Amjady, A. Baharvandi, M. A. Akbari, “Generation and transmission expansion planning: MILP-based probabilistic model,” IEEE Trans. Power Syst, vol. 29, no. 4, pp. 1592–1601, 2014.
- [21] D. Bertsimas, E. Litvinov, X. A. Sun, J. Zhao, and T. Zheng, “Adaptive robust optimization for the security constrained unit commitment problem,” IEEE Trans. Power Syst., vol. 28, no. 1, pp. 52-63, Feb. 2013.
- [22] S.A. Bozorgavari, J. Aghaei, S. Pirouzi, A. Nikoobakht, H. Farahmand, M. Korpås, “Robust planning of distributed battery energy storage systems in flexible smart distribution networks: A comprehensive study,” Renewable and Sustainable Energy Reviews, vol. 123, pp. 109739, 2020.
- [23] C.A. Saldarriaga, R.A. Hincapié, H. Salazar, “A Holistic Approach for Planning Natural Gas and Electricity Distribution Networks,” IEEE Transactions on Power Systems, vol. 28, no. 4, pp. 4052-4063, 2014.
- [24] [Online]. Available: <https://sites.google.com/site/chengwang0617/home/data-sheet>.
- [25] S. Abrisham Foroushan Asl, M. Gandomkar, J. Nikoukar, “Optimal protection coordination in the micro-grid including inverter-based distributed generations and energy

- storage system with considering grid-connected and islanded modes,” *Electric Power Systems Research*, vol. 184, pp. 106317, 2020.
- [26] Nord Pool, <https://www.nordpoolgroup.com/historical-market-data/>.
- [27] Generalized Algebraic Modeling Systems (GAMS). [Online]. Available: <http://www.gams.com>.
- [28] M. Shahidehpour, H. Yamin, Z. Li, “Market operations in electric power systems: forecasting, scheduling, and risk management,” Wiley-IEEE Press, 2002.
- [29] “Reliability test system task force, the IEEE reliability test system 1996,” *IEEE Trans. Power Syst.*, vol. 14, no. 3, pp. 1010–1020, Aug. 1999.